T.R.
GEBZE TECHNICAL UNIVERSITY
INSTITUTE OF BIOTECHNOLOGY

INVESTIGATION OF POLYDOPAMINE MODIFICATION ON SURFACE PLASMON RESONANCE SENSOR CHIP FOR DETECTION OF BIOMOLECULES

ÖZGE ÇELİK
A THESIS SUBMITTED FOR THE DEGREE OF
MASTER OF SCIENCE
DEPARTMENT OF BIOTECHNOLOGY

GEBZE
2021

T.R.

GEBZE TECHNICAL UNIVERSITY

INSTITUTE OF BIOTECHNOLOGY

INVESTIGATION OF POLYDOPAMINE COATING ON SURFACE PLASMON RESONANCE SENSOR CHIP FOR DETECTION OF BIOMOLECULES

ÖZGE ÇELİK

A THESIS SUBMITTED FOR THE DEGREE OF MASTER OF SCIENCE

DEPARTMENT OF BIOTECHNOLOGY

THESIS SUPERVISOR

ASST. PROF. MUHAMMED ENES ORUÇ

GEBZE

2021

T.C.
GEBZE TEKNİK ÜNİVERSİTESİ
BİYOTEKNOLOJİ ENSTİTÜSÜ

BİYOMOLEKÜLLERİN TESPİTİ İÇİN YÜZEY PLAZMON REZONANS SENSÖR ÇİPİNDE POLİDOPAMİN MODİFİKASYONUNUN İNCELENMESİ

ÖZGE ÇELİK

YÜKSEK LİSANS TEZİ
BİYOTEKNOLOJİ ANABİLİM DALI

DANIŞMANI
DR. ÖĞR. ÜYESİ MUHAMMED ENES ORUÇ

GEBZE
2021

GEBZE TEKNİK ÜNİVERSİTESİ	YÜKSEK LİSANS JÜRİ ONAY FORMU

GTÜ Biyoteknoloji Enstitüsü Yönetim Kurulu'nun 14/06/2021 tarih ve 2021/14 sayılı kararıyla oluşturulan jüri tarafından 18/06/2021 tarihinde tez savunma sınavı yapılan ÖZGE ÇELİK'in tez çalışması Biyoteknoloji Enstitüsü YÜKSEK LİSANS tezi olarak kabul edilmiştir.

JÜRİ

ÜYE
(TEZ DANIŞMANI) : Dr. Öğr. Üyesi Muhammed Enes ORUÇ

ÜYE : Dr. Öğr. Üyesi Özgün YÜCEL
Gebze Teknik Üniversitesi, Kimya Mühendisliği

ÜYE : Doç.Dr. Cem Bülent ÜSTÜNDAĞ
Yıldız Teknik Ünivesitesi, Biyomühendislik

ONAY

Gebze Teknik Üniversitesi Biyoteknoloji Enstitüsü Yönetim Kurulu", nun
…..…/…..…/..…… tarih ve ……/…….. sayılı kararı.

İMZA/MÜHÜR

SUMMARY

Surface plasmon resonance is a sensitive optical technique used to detect molecular interactions as a surface-oriented method. Up to now, many materials and methods have been developed to increase signal amplification and the amount of protein immobilized to the sensor surface. One of the materials used for surface modification is Polydopamine (PDA). PDA is a very suitable material for surface modification studies due to its easy application and versatile properties such as being able to adhere to almost any solid substrate. In particular, PDA is attracting attention as a versatile functional coating material in various bio-related devices for biomolecule immobilization. PDA films have a rough surface. However, the effect of surface roughness and thickness of PDA films on protein binding remains unclear. In this study, the kinetics of protein-PDA interaction were investigated and the effect of surface roughness and film thickness on protein binding was investigated. At the end of this study, it was found that as the thickness of the PDA film increased, the surface roughness and particle size increased. However, it was observed that there was no significant difference in protein immobilization capacity at different PDA film thicknesses. This work can deepen our understanding of PDA-protein interaction and provide a valuable guide for efficient protein binding to PDA film in a variety of bio-related applications.

Keywords: Polydopamine (PDA), surface plasmon resonance (SPR), protein attachment, roughness, PDA film, surface modification.

ÖZET

Yüzey plazmon rezonansı, yüzey odaklı bir yöntem olarak moleküler etkileşimleri tespit etmek için kullanılan hassas bir optik tekniktir. Şimdiye kadar, sinyal amplifikasyonunu ve sensör yüzeyine hareketsizleştirilmiş protein miktarını artırmak için birçok malzeme ve yöntem geliştirilmiştir. Yüzey modifikasyonu için kullanılan malzemelerden biri Polydopamine'dir (PDA). PDA, kolay uygulaması ve hemen hemen her katı alt tabakaya yapışabilme gibi çok yönlü özellikleri nedeniyle yüzey modifikasyon çalışmaları için çok uygun bir malzemedir. Özellikle PDA, biyomolekül immobilizasyonu için çeşitli biyo-bağlantılı cihazlarda çok yönlü işlevsel bir kaplama malzemesi olarak dikkat çekmektedir. PDA filmleri pürüzlü bir yüzeye sahiptir. Bununla birlikte, PDA filmlerinin yüzey pürüzlülüğünün ve kalınlığının protein bağlanması üzerindeki etkisi belirsizliğini korumaktadır. Bu çalışmada, protein-PDA etkileşiminin kinetiği incelenmiş ve yüzey pürüzlülüğünün ve film kalınlığının protein bağlanması üzerindeki etkisi araştırılmıştır. Bu çalışmanın sonunda, PDA filminin kalınlığı arttıkça yüzey pürüzlülüğünün ve parçacık boyutunun arttığı bulunmuştur. Bununla birlikte, farklı PDA film kalınlıklarında protein immbolizasyon kapasitesinde önemli bir fark olmadığı gözlenmiştir. Bu çalışma, PDA-protein etkileşimi konusundaki anlayışımızı derinleştirebilir ve çeşitli biyo ile ilgili uygulamalarda PDA filme verimli protein bağlanması için değerli bir kılavuz sağlayabilir.

Anahtar kelimeler: Polidopamin (PDA), Yüzey plazmon rezonans, protein bağlanması, PDA film, yüzey modifikasyonu.

ACKNOWLEDGEMENTS

I would like to express my gratitude to my supervisor, Asst. Prof. Muhammed Enes ORUÇ, who shared his scientific knowledge with me, supported and encouraged me during this research.

I want to thank my parents, mother, father, and my sisters, for their bottomless love, support. I could not have done this without them.

I would like to thank Dr. Kübra Erdoğar for sharing all her experiences and advices with me.

Also, I want to thank my cousins Beyza Nur Çelik and Ayse Sena Çelik and my best friend Şüheda Saruhan for their supporting and encouragement.

This study was supported by the Scientific and Technological Research Council of Turkey (TUBITAK) Grant No: 217M221.

TABLE of CONTENTS

LIST of ABBREVIATIONS and ACRONYMS

Abbreviations and Acronyms		Explanations
AgNPs	:	Silver nanoparticles
C	:	Constant concentration of analyte
k_a	:	Association rate constant in M^{-1} s^{-1}
k_d	:	Dissociation rate constant in s^{-1}
K_D	:	Equilibrium constant in Molar
MoS_2	:	Molybdenum disulfide
R_{max}	:	Maximal response in RU
R_{eq}	:	Equilibrium response in RU
SiO_2	:	Silicon dioxide, quartz
AFM	:	Atomic force microscopy
BSA	:	Bovine serum albumin
CMD	:	Carboxymethylated dextran matrix
DA	:	Dopamine
DNA	:	Deoxyribonucleic acid
IgG	:	Immunoglobulin G
IL-6	:	Interleukin-6
MIF	:	Macroporous molecularly imprinted film
NHS	:	N-hydroxysuccinimide
PDA	:	Polydopamine
Ra	:	Roughness average
RI	:	Refractive index
RU	:	Resonance (response) unit
SAM	:	Self-assembled monolayers
SPR	:	Surface plasmon resonance
TIR	:	Total internal reflection
QCM	:	Quartz crystal microbalance

LIST of FIGURES

LIST of TABLES

1. INTRODUCTION

1.1. Motivation

Surface plasmon resonance (SPR), an optical technique, is used for detecting molecular interactions, such as proteins, bacteria, or other classes of molecules. This optical method is based on the measurement of refractive index changes associated with the interaction between target analytes and attached biomolecular recognition components on the sensor surface. SPR is a rapid and sensitive approach for detecting biomolecular interactions that is label-free and in real time. Therefore, SPR is widely employed in a variety of fields, including environmental protection, biotechnology, medical diagnostics, drug screening, food safety, and security [1].

The sensor chip's surface has an enormous effect on the biosensor's performance and sensitivity and the quality of the data retrieved. The sensor chip covered with a thin metal layer (e.g., gold, silver) is not sufficient for the adsorption of proteins onto the sensor surface. Therefore, diverse sensor surfaces have been developed for the immobilization of proteins [2]. One approach is to create porous structures on the sensor surface. Porosity on the surface increases surface area, and thus, it provides attachment of a higher amount of proteins to the sensor surface. Also, it could enhance the sensitivity since it improves binding capacity. Thus, it provides the target analytes to attach swiftly to the sensor surface. Zhang et al. developed a water-compatible macroporous molecularly imprinted film (MIF) that uses surface plasmon resonance to detect testosterone. They discovered that MIF's high porosity increases its accessibility and sensitivity to testosterone binding, and that macroporous MIF has superior selectivity than normal MIF for recognizing testosterone molecules. [3]. In another study, Rahman et al. investigated the performance of porous silicon-based SPR sensors using graphene-MoS_2 hybrid structure. They found that this hybrid structure on porous silicon sensor has 25% more sensitivity than the conventional silicon resonant sensor [4]. Another approach is to modify surfaces with various molecules. The surface chemistry of the sensor chip is essential for the adsorption of proteins onto the sensor surface. One of the surface chemistry modifications is provided by polydopamine (PDA). PDA is organized on the surfaces by the self-polymerization of dopamine (DA), a catecholaminergic biological neurotransmitter, at alkaline pH

values. The catechol, amine, imine, and quinone groups are all present in PDA. These groups enable binding with a diverse biomolecules without the need for any additional surface activation or treatment. PDA also outperforms traditional coupling agents like N-hydroxysuccinimide (NHS) or maleimide in terms of hydrolysis resistance and conjugation proficiency. Up to now, PDA coated surfaces have been suggested on various applications, which are cell adhesion, control wettability of surfaces, anti-biofouling surfaces, and biosensors.

Toma and Tawa [5] investigated the utilization of polydopamine thin films as protein linker layer for sensitive detection of Interleukin-6 by surface plasmon resonance (SPR) biosensor. Interleukin-6 (IL-6) was detected by utilizing sandwich immunoassay. They used recombinant anti-human IL-6 antibody as a capture antibody for the detection of IL-6. They found that the PDA coated sensor chips demonstrated sensitive sensor responses of the detection antibody on the sensor surface. Wang et al. [6] studied a novel surface plasmon resonance biosensor based on the PDA-AgNPs-PDA-Au film sensing platform for horse IgG detection. They used polydopamine as a sensor surface for detection of horse IgG detection. They found that the sensor chip is remarkably stable and regenerative. Yang et al. [7] investigated the stability of the PDA which coated on gold surfaces under a variety of circumstances. They did this by experimenting with ten different organic solvents to change the pH of aqueous solutions from 1 to 14. They also looked into the influence of the thickness of the PDA coated surface on the SPR signal. They discovered that when PDA is deposited on sensor surfaces, SPR signals rise. As a result, they obtained systematic and extensive information on the stability and reactivity behaviors of PDA coatings. Chen et al. [8] investigated protein immobilization on PDA film using a real-time and label-free surface plasmon resonance (SPR) method. The effect of buffer pH and deposition media on protein immobilization was explored, as well as the kinetics of protein-PDA surface contact.. They demonstrated that PDA film was steady of protein immobilisation, and PDA coated surface has high protein immobilisation capability. They found that the SPR angle increased from 70 to 85 degree when the PDA film thicknesses increase from 0 to 60 nm. They exhibited that when the PDA film thickness was 40 nm or above, the minimum reflectivity (resonance depth) and curve shape (resonance width) both rose significantly, resulting in a lower SPR signal-to-noise ratio.

1.2. The Objective of the Thesis

The thesis aims to investigate the improvement of SPR signal at different PDA thicknesses coated on SPR biosensor chips. We hypothesize that a thicker PDA layer with a higher surface area may increase the binding quantity of analytes, and the SPR signal may increase. The objectives of the thesis are to:

- Deposit PDA layers on gold coated glass substrate at different thickness, leading to various roughness,
- Perform SPR analysis with the target molecule and investigate the binding quantity of the molecules on different PDA layer thicknesses.

1.3. The Scope of the Thesis

In this study, we have chosen polydopamine (PDA) since it is easy to use, cost-effective, and has a short deposition time, and does not require any coupling agents as a detection interface for the surface plasmon resonance biosensor. Deposition of different PDA thicknesses on gold coated glass substrate was provided. The morphological and physical properties of the substrates were characterized. Finally, SPR analyses were performed on the prepared SPR biosensor chips.

2. BACKGROUND

2.1. What is a Biosensor?

Biosensors can be described as an analytical devices to detect or analyze a target by a transducer. A biosensor device generally consists of three basic components: (1) a biological recognition system, also known as a bioreceptor, (2) a transducer, and 3) microelectronics. A biosensor's primary premise is to detect molecule contact and convert it into a measurable signal, such as an electrical/ optical signal, using a transducer [9]. A biosensor's goal is to provide fast, accurate, and dependable information in real time. In medical, food safety, agriculture, pharmaceuticals, bioprocessing, environmental, industrial monitoring, and biodefense, biosensors play a significant role. [9], [10]. The first biosensor is designed to measure glucose concentration by Clark and Lyons in 1962. They measured glucose concentration by binding glucose oxidase to the amperometric oxygen electrode surface [11].

2.2. Basic Principles of Biosensors

The term biosensor is the abbreviation of a biological sensor. The main principle of a biosensor is depicted in Figure 2.1. A biosensor device comprises a transducer and a biological molecule such as nucleic acid, antibody, enzyme, DNA, cell, bacteria, and virus. A biological reaction occurs when these molecules interact with the analyte being examined. The transducer converts this biological response into an electrical signal. When the analyte is attached to the biological molecule, a chemical reaction occurs due to the interaction of these. The chemical reaction can produce new molecules, charge flow, heat release, mass, and pH change. This chemical reaction is detected and converted to a measurable electronic response by the transducer [9], [11]. Eventually, the electrical signal is transferred as a response to a computer workstation [12]. The type of sensor where the biological molecule binds to the analyte is named “affinity biosensor”. Sensors in which a biological component and an analyte induce chemical changes that can quantify a concentration of substrate are named "metabolic biosensors". The type of sensors where a biological l component reacts with the analyte

and changes it into an assistance substrate rather than changing it chemically is named "catalytic biosensors" [9].

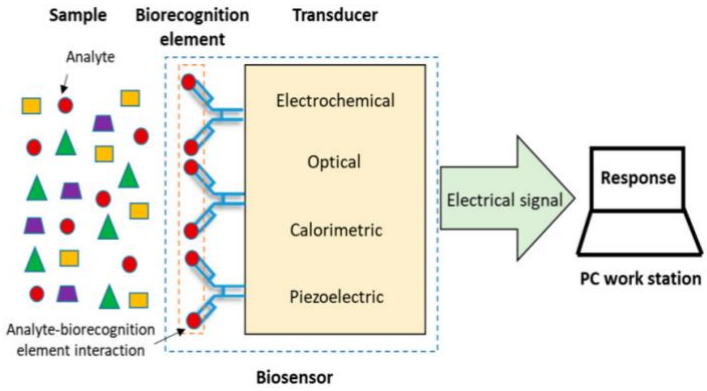

Figure 2.1: Component of a biosensor (Contreras-Naranjo and Aguilar, 2019)

2.3. Classification of Biosensors Based on Transducers

The transducer is a biosensor element that aids in the conversion of biorecognition signal events to detectable signals. The biosensors are classified as optical, electrochemical, calorimetric and piezoelectric sensors according to their transducers type.

2.3.1. Electrochemical Biosensors

Biosensors containing an electrochemical transducer are called electrochemical biosensors. In this biosensor type, an electrode is used as the transduction component. An electrochemical biosensor, according to the 1999 IUPAC definition, is a self-contained integrated device that uses a biological recognition compound in direct communication with an electrochemical transduction component to provide particular quantitative or semi-quantitative analytical information.. An electrochemical biosensor quantifies the stream resulting from oxidation and reduction reactions. Electrochemical biosensors are frequently used in the biological analysis because it supplies information about the content/density of the analyte of interest by enabling the direct conversion of a biological incident into an electrical signal. Electrochemical biosensors can be classified as potentiometric, conductometric, amperometric, or

voltammetric biosensors based on the type of electrical property detected and measured. Transportable, simple, easy to use, cost-effective, and, in most cases, disposable electrochemical transducers are frequently chosen. Electrochemical biosensors have been reduced to pocket-sized devices that can be used at home or in clinical settings. Last but not least, electrochemical biosensors are inexpensive. All of these facts encourage us to explore the subject of electrochemical biosensors. [9].

2.3.2. Calorimetric Biosensors

Heat exchange occurs as a result of all chemical and biological reactions [13]. The calorimetric-based biosensors are also founded on the concept of heat generation and absorption happening in all metabolic reactions. Calorimetric transduction was first used for enzyme-based sensors, then for DNA/cell and immunosensors. Calorimetric (enthalpy metric) biosensors quantify the heat formation in biochemical reactions, i.e., the enthalpy change. The number of reactants consumed or the products generated can both contribute to the temperature change. A thermistor (often metal oxide) or a thermophile (typically ceramic semiconductor) is used to measure heat change in calorimetric devices. In most calorimetric biosensors, immobilized enzymes are used on the carrier free in solution or accommodated on the thermistor surface or in the reactor. These thermal sensors have advantages such as stability, increased sensitivity, and the possibility of miniaturization. With a calorimetric biosensor, DNA hybridization can be detected quickly. Today, calorimetric biosensors are utilized in the food industry and environmental monitoring [9], [14].

2.3.3. Piezoelectric Biosensors

The piezoelectric effect was discovered in 1880 by the Curie brothers (the younger brother, Pierre, was Marie Curie’s husband). They discovered that when quartz is compressed or stretched, an electric voltage is generated (Figure 2.2). This influence is reversible, which means that when an electrical voltage is supplied, quartz can be prolonged or shortened. Piezoelectricity refers to a material's capacity to demonstrate the piezoelectric effect [15]. Because of its unique tetrahedral crystal structure, quartz (SiO_2) is still the most popular and commonly used material for

piezoelectric sensors, despite the fact that tourmaline, lithium niobate, and aluminum nitride also display piezoelectricity [11], [15]. AT-cut quartz discs which are 10–15 mm diameter and 0.1–0.2 mm thickness, are the most favorite commercial quartz crystal microbalance (QCM) crystals. These discs are coated with gold or silver thin film electrodes [16], [17].

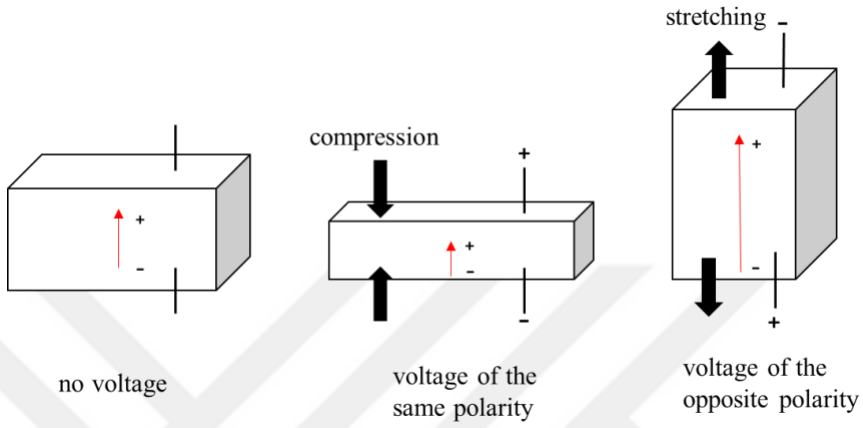

Figure 2.2: Piezoelectric effect of an AT-cut quartz crystal.

2.3.4. Optical Biosensors

Optical biosensors are sensitive detection and analysis devices utilized in biomedical research, diagnostics, pharmaceuticals, healthcare, and biodefense. The transduction process, which is the most common type of optical biosensor, causes a change in phase, amplitude, polarization, or frequency of the input light in response to physical or chemical changes created by the bio-recognition process. Optical biosensors have some advantages: selectivity, rapid, real-time, label-free, compact design, minimally invasive for in vivo measurements, biocompatible optical elemens, multiple channels/multi parameters detections, ensuring detailed chemical information on analytes. A light source, optical transmission medium (fiber, waveguide, etc.), immobilized biological recognition components (enzymes, antibodies, or microorganisms), and an optical detection system make up an optical biosensor [9]. There are different optical biosensors, such as UV-vis absorption, fluorescence, chemiluminescence / bioluminescence, surface plasmon resonance, reflection spectroscopy, and laser light scattering [11].

Fluorescence-based biosensors

One of the most sensitive spectroscopic techniques, fluorescence, is ideal for examining biomolecules. Very low concentrations of biomolecules can be detected with fluorescence sensors. Fluorescence is often used for signal transduction, particularly in enzyme and antibody-based studies. Fluorescence sensors require an external light (short-wavelength light) source to start electronic transitions in an atom or molecule, resulting in luminescence (light with a longer wavelength) is generated [9]. Mineral fluorite containing calcium fluoride is used in fluorescence sensors, and the term fluorescence comes from here [15]. Most biological elements and analytes do not have intrinsic spectral features. Therefore, optically sensitive fluorochrome molecules are attached to sensing elements and converted into an optical signal in the fluorescence-based biosensors. This method is utilized to generate light during the biorecognition event. For example, nucleic acids, antibodies, cells are labeled with fluorochrome to generate an optical signal. Fluorescence biosensors are also used to transform the hybridization interaction between two strands of DNA into optical signals. The disadvantage of this method is that fluorescent sensors are not appropriate for real-time monitoring. By fluorescence spectroscopy, very low analyte concentrations can be detected with fluorescence emission intensity. Therefore, it is a sensitive technique. Fluorescent materials and fluorescent dyes are used to generate light signals in the fluorescent biosensor construction [9]. Fluorescent dyes such as DAPI, Fluorescein, Rhodamine B, Cy5, Cy3, and advanced fluorescent dyes such as GFP, SYBR, QD are frequently used in chemical and biological applications [15].

Chemiluminescence-based biosensors

Chemiluminescence is one of the most sensitive analytical chemistry techniques. Light can be emitted in the ultraviolet, visible, or infrared ranges in this method. The chemiluminescence method is based on the formation of electromagnetic radiation in the form of light by releasing energy from a chemical reaction. It is one of the most beneficial and widely optical detection methods in terms of instrumentation and applicability [14].

Chemiluminescent reactions are classified according to the nature of the reactions that initiate light emission as chemiluminescent, bioluminescent, and

electrochemiluminescent reactions. Reactions of synthetic components containing strong oxidants are called chemiluminescent reactions, e.g., Cerium (IV) salt and peroxide reactions. The luminescence that occurs with the help of a particular protein or enzyme that occurs in some living organisms (firefly or jellyfish) is called bioluminescent reactions. Studies on microorganisms made by genetic engineering with the luciferase enzyme and luciferase gene (lux) are also bioluminescent. Luminescent reactions that occur with electric current are called electrochemiluminescent reactions [14], [17].

It was realized that luminescent reactions are appropriate transducers to design precise optical biosensors. Lately, chemiluminescence and electrochemiluminescence detection methods have been utilized in the development of biochip and microarray biosensors [9].

2.4. Surface Plasmon Resonance

Surface plasmon resonance (SPR) is an optical method used to detect molecular interactions. Surface plasmons were discovered by Wood in 1902. Wood saw a pattern of "abnormal" dark and light bands in reflected light when he shone polarized light onto a mirror with a diffraction grating on its surface. Lord Rayleigh pioneered the physical interpretation of the event, which was later elucidated by Fano. However, Otto and Kretschmann and Raether announced in before 1968 that surface plasmon excitation fully explained the behavior. Liedberg et al. showed the use of SPR-based sensors to monitor biomolecular interactions in 1983. [18].

When the target analyte interacts with the biosensing element on the sensor, surface plasmon waves (electromagnetic waves) are used to detect changes on the sensor surface by SPR biosensors. The binding of a moving molecule (analyte) to the molecule (ligand) immobilized on a thin metal film surface changes the refractive index of the sensor metal film. Through SPR biosensors, interactions between biomolecules such as proteins, antibodies, antigens, nucleic acids, and enzymes can be monitored unlabeled and in real time without any radioactivity and fluorescence. Therefore, label-free, real-time, anti-interference ability, samples without pretreatment, fast, high throughput analysis, fewer reagents, and samples are advantages of surface plasmon resonance biosensors [9].

SPR has physical as well as biological applications. SPR is used to assess dielectric properties, adsorption processes, surface degradation of thin organic monolayers/bilayers, and polymer films in physical applications. SPR is also employed in biological sensing applications. SPR biosensors can detect specific biological interactions involving adsorption and desorption kinetics, antigen-antibody binding, and epitope mapping to determine biomolecular structure and interactions of proteins, DNA, bacteria, and viruse [9].

2.4.1. Phenomenon of Surface Plasmon Resonance

The SPR phenomenon is mainly based on total internal reflection (TIR). Total internal reflection occurs at an interface between non-absorbent media. When a light-emitting beam in a medium with a higher refractive index encounters an interface with a lower refractive index, the light is fully reflected at the interface and propagated back into the medium with a high refractive index (Figure 2.3). The evanescent field is a non-transverse wave with components in all spatial orientations and decreases in field density by penetrating the metal medium. However, its energy is an oscillating electrical or magnetic field spatially concentrated in the vicinity where the SPR effect occurs. The TIR interface is coated with a layer of an appropriate conducting metal material. For a non-magnetic metal, usually gold, this surface plasmon wave will also be p-polarized and, owing to its electromagnetic and surface propagating nature, will compose an improved evanescent wave [19], [20], [21].

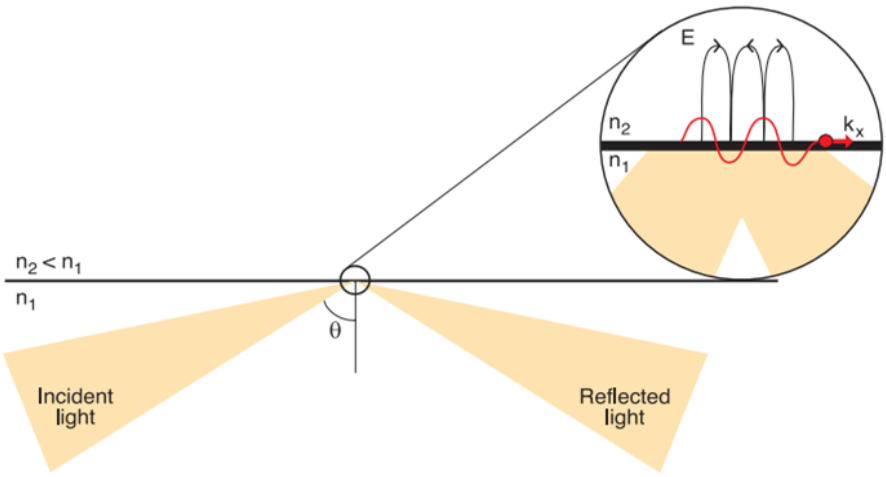

Figure 2.3: TIR for non-absorbing media. Light is emitted at the interface n_1, subjected to total internal reflection with the medium having a lower refractive index n_2. The evanescent field is a non-transverse wave that enters the n_2 environment and decreases the field density. θ is the angle of incidence (Biacore).

When polarized light travels through a prism on a sensor chip covered in a thin metal film, the metal film reflects the light like a mirror. At a certain angle of incidence, p-polarized light photons interact with free electrons of the metal surface, and energy is transferred to the electrons of the metal. This energy transfer generates surface plasmon polaritons at the metal-medium interface. In consequence of the energy transfer, there is a decline in reflected light intensity (gray zone) at a given angle of incidence (Figure 2.4) [9].

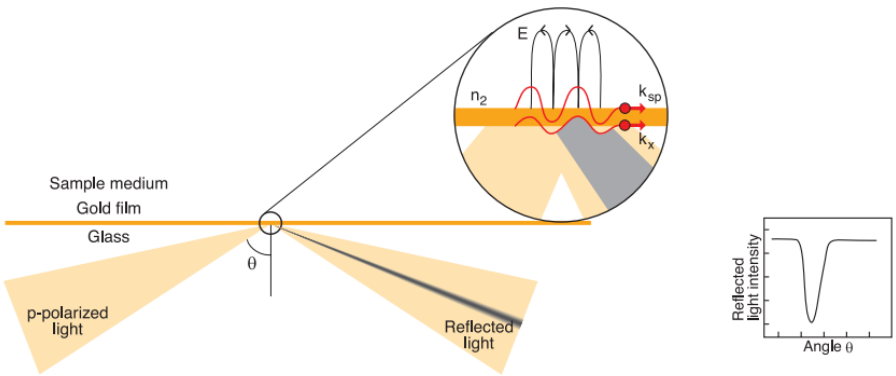

Figure 2.4: At a glass/metal film interface, p-polarized fully internally reflected light induces SPR, with the surface plasmon enhancing the evanescent field amplitude, E (Biacore).

2.4.2. Principle of Surface Plasmon Resonance

Figure 2.5. depicts the operating principle of the SPR measurements. The molecules (analytes) are released through a flow channel onto the gold-plated sensor chip on a prism and immobilized to the sensor surface. The light source on the sensor chip emits polarized light. Surface plasmons are excited at a given angle of incidence, causing the angle of reflected light to decrease. The detector monitors this density drop. The resonance angle, also known as the SPR angle, is the maximum decrease in the intensity of reflected light. The angle shift from I to II is caused by a change in the refractive index at the gold film's surface. In a typical SPR biosensor, this resonance angle change is displayed in a sensorgram as the sensor signal. This change in the SPR angle is approximately equivalent to the mass of molecules adsorbed. An angle change of 0.1 degrees corresponds to a change in response units of 1000 that is equivalent to surface mass [9], [22], [23].

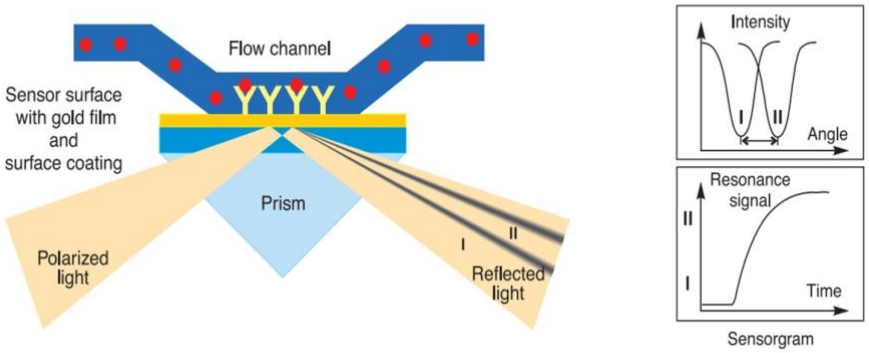

Figure 2.5: Surface plasmon resonance principle.

2.4.3. Mass Transport Limitation

Mass transport is the process of diffusing an analyte from a bulk solution onto the biosensor chip surface. Mass transport is a commonly known limitations for calculating the rate of association constant. If the binding curves differ when a constant analyte concentration is injected at different flow rates, this interaction is limited by mass transport. These problems may be prevented by immobilizing a low quantity of ligand (50-150 RU) and performing the binding analysis at a high flow rate

(30-100 μL min^{-1}). Equation (1.1) can be used to calculate the quantity of ligand immobilized on the surface.

$$R_{Ligand} = \frac{R_{max} \cdot R_{Ligand} \cdot v_{Ligand}}{M_{Analyte}} \quad (2.1)$$

where $M_{Ligand/Analyte}$ is the corresponding molecular weight, v_{Ligand} the valency of the ligand, and R_{Ligand} the quantity of immobilized ligand in RU (resonance unit) [25], [28].

2.4.4. Binding Kinetics Analysis

During SPR analysis, as analytes bind to the ligand, the mass on the sensor surface increases, resulting in an increment in the refractive index. This change in refractive index may be detected in real time with SPR. The result is plotted in units of response versus time (RUs). The graph with these results is called a sensorgram. It shows the real-time progress of the interaction on the sensor surface. The signal is proportional to how many molecules are attached to the sensor surface. In most SPR devices, a signal of 1000 RUs equates to 1 ng/mm-2 protein. As a result, SPR is appropriate for providing information on biomolecule binding kinetics, such as protein adsorption on the surface. [24].

The sensorgram demonstrates the binding kinetics of biomolecules in three stages (Figure 2.6). The first stage is the association stage, in which analytes bind to the ligand, increasing the number of RUs. The association ratio is calculated using the curve that results (k_a). The second stage, known as the association stage, determines the rate of compound creation over time. This stage is at a steady state where the association/dissociation events are equal. This stage is at a steady state, with an equal number of association and dissociation events. The amount of RUs obtained during this equilibrium phase is referred to as an equilibrium response (R_{eq}), and it is used to calculate binding affinity (K_D). The disassociation phase begins when the analyte injection through the flow cell is stopped: the analyte departs the surface while the working buffer flows over the chip. The number of RUs decreases when the analyte is separated from the ligand-binding site. The dissociation rate is measured using the accompanying curve (k_d). During the regeneration stage, the analyte is totally moved

away from the ligand-binding sites, and the surface becomes ready for further injection cycles. [25].

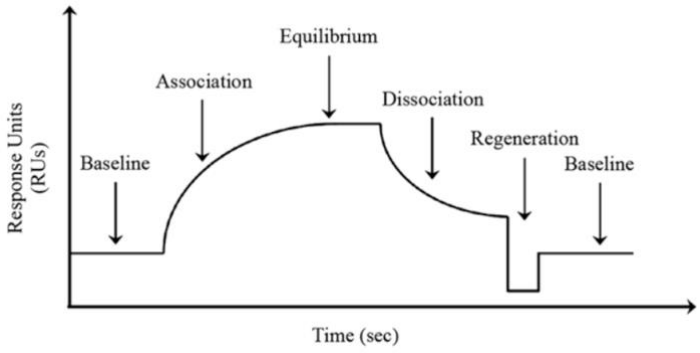

Figure 2.6: Association/disassociation sensorgram of SPR (Douzi B., 2017).

SPR can monitor the reaction rate and equilibrium constants of a chemical interaction where A is the analyte and B is the ligand immobilized at the sensor surface, e.g., A + B → AB. At a unit concentration of A and B, the association constant is the reaction rate that gives the number of AB compounds created per time. When AB compounds are established, dissociation may also begin. Dissociation constant defines that this process and represents the number of AB compounds that decompose per unit time. The unit sizes for association and dissociation rates differ and can alter depending on the stoichiometry of the compound [15]. Table 2.1 includes the most convenient kinetic parameters, the association and dissociation constants, for the most basic case A+B→AB (Tudos A. J. and Schasfoort R. B. M., 2008).

Table 2.1: Descriptions of the most convenient kinetic parameters: the association and dissociation constants.

	Association rate constant, k_a	Dissociation rate constant, k_d
Definition	A + B → AB	AB → A + B
Explanation	Reaction rate of AB formation: amount of AB compounds formed per unit time at unit concentration of A and B	Dissociation rate of AB: amount of AB compounds dissociating per unit time
Units	$l\ mol^{-1}\ s^{-1}$	s^{-1}
Typical range	$10^3 - 10^7$	$10^{-1} - 5 \times 10^{-6}$

The equilibrium association and dissociation constants indicating the affinity of interaction can be seen to have a bilateral relationship with each other. Furthermore, affinity and rate constants in an interaction depend on experimental conditions such as temperature, pH, and buffer composition. Therefore, these conditions should be considered when determining affinity and rate constants [26]. The equilibrium constants of molecular interactions are given in Table 2.2 (Tudos A. J. and Schasfoort R. B. M., 2008).

Table 2.2: Descriptions of the equilibrium constants of molecular interactions.

	Equilibrium association constant, k_a	Equilibrium dissociation constant, k_d
Definition	[AB] / [A][B] = k_a / k_d	[A][B] / [AB] = k_d / k_a
Explanation	Affinity to association: high k_a, high affinity to associate	Stability of AB: high k_d, low stability of AB
Unit	l mol^{-1}	mol l^{-1}
Typical range	$10^5 - 10^{12}$	$10^{-5} - 10^{-12}$

The simplest model to explain the kinetic principle of the interaction between an analyte-ligand is the Langmuir model. This model depicts a 1:1 interaction between a ligand and an analyte molecule, as in Figure 2.7. The association constant k_a represents the rate of formation of the complex, whereas the dissociation constant k_d represents the rate of separation of the complex.

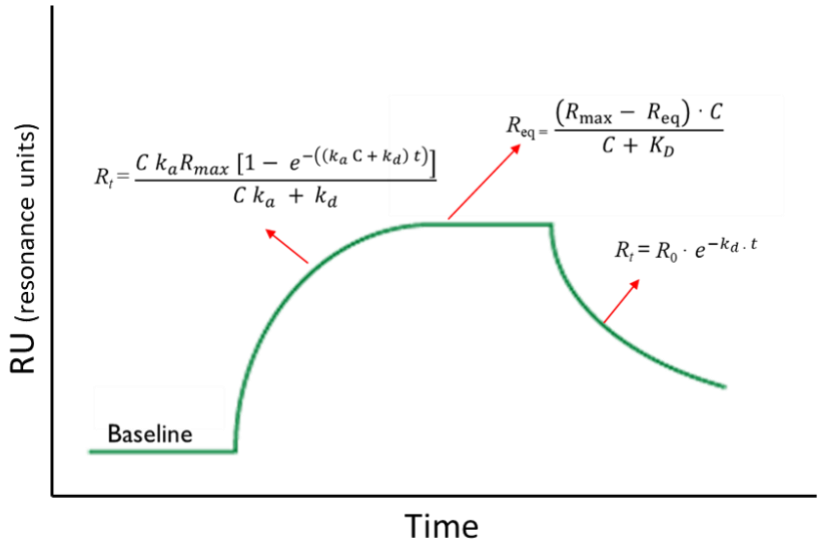

Figure 2.7: The sensorgram phases.

The reversible interaction can be described by a basic equation display below:

$$A + B \underset{k_d}{\overset{k_a}{\leftrightarrow}} \mathrm{AB} \tag{2.2}$$

The following differential equation can be used to express the rate of production of the product, AB, at time *t*:

$$\frac{d[AB]}{dt} = k_a\,[A]\,[B] - k_d\,[AB] \tag{2.3}$$

where [A] and [B] are the corresponding molar concentrations of free or unbound analyte and ligand, respectively. After some reaction time, *t*, $[B]_0 - [B] = [AB]$, where $[B]_0$ is the concentration of B at $t = 0$. Substituting this equation into Eq. (2.3) gives:

$$\frac{d[AB]}{dt} = k_a\,[A]\,([B]_0 - [AB]) - k_d\,[AB] \tag{2.4}$$

The observed signal, *R*, is commensurate to the creation of AB compounds at the surface and the maximum signal, R_{max}, will be proportional to the surface concentration of active ligand at the surface. Consequently, in the case of an SPR experiment, Eq. (2.4) can be written as:

$$\frac{dR}{dt} = k_a\,C\,(R_{max} - R)\,k_d - R \tag{2.5}$$

where *dR / dt* is the rate of generation of surface associated complexes, i.e., the derivative of the monitored response curve, *C* is the constant concentration of analyte in solution. R_{max} is the capacity of the immobilized ligand on the chip surface described in resonance units, and (R_{max} - *R*) is equivalent to the number of blank surface binding sites at time *t* [27]. If Eq. (2.4) and Eq. (2.5) are combined:

$$R_t = \frac{C\,k_a R_{max}\,[1 - e^{-\left((k_a\,C + k_d)\,t\right)}]}{C\,k_a + k_d} \tag{2.6}$$

Steady state: there are two ways to calculate the equilibrium dissociation constant K_D. K_D can be computed using the ratio of the association and dissociation constants acquired from kinetic analysis in the first technique:

$$K_D = \frac{k_a}{k_d} \tag{2.7}$$

Response units in equilibrium at varying analyte concentrations are utilized in the second method. The dissociation constant is calculated using nonlinear regression on the acquired saturation curve:

$$\frac{dR}{dt} = k_a\,(R_{\max} - R_{\text{eq}}) \cdot C - k_d \cdot R_{\text{eq}} = 0 \tag{2.8}$$

$$\Longleftrightarrow R_{\text{eq}} = \frac{(R_{\max} - R_{\text{eq}}) \cdot C}{C + k_a/k_d} = \frac{(R_{\max} - R_{\text{eq}}) \cdot C}{C + K_D} \tag{2.9}$$

where R_{eq} is the steady-state response and C is the analyte concentration [28].

After the analyte passing through the flow cell is stopped, the dissociation phase takes place. The analyte moves away from the surface as the buffer solution flows over the surface of the chip. The dissociation process of the formed complexes can be observed directly. The rate of dissociation AB of the formed complexes is defined as:

$$\frac{dR}{dt} = - k_d \cdot R \tag{2.10}$$

The linearized form of Eq. (2.10) is:

$$\ln \frac{R_0}{R_t} = k_d \cdot (t - t_0) \tag{2.11}$$

where R_0 is the response at t_0 and R_t is the response at time $t = n$ along the dissociation curve. If the results obtained follow the 1: 1 kinetic model, a plot of $\ln(R_0 - R_t)$ and $(t_0 - t)$ produces a linear k_d slope line.

$$R_t = R_0 \cdot e^{-k_d \cdot t} \tag{2.12}$$

2.5. SPR Chips and Surface Chemistry

The immobilization of biological recognition elements to a sensor chip surface is a very important part of building biosensors. The molecular structure of the detection interface is one of the essential issues to be considered in SPR analyzes. The sensor chip surface has a significant impact on the performance, sensitivity of an SPR biosensor, and quality of the received data. Depending on the application, several design issues must be considered, including the surface receptor to target the desired analyte and the process of binding that receptor to active material. A biosensor chip usually consists of the glass substrate covered with a thin metal layer (usually gold), which provides surface plasmons to be stimulated. Direct adsorption of biomolecules on metal surfaces can induce denaturation of biomolecules and block ligand binding sites due to their random orientation on the metal surface. Furthermore, because of the weak connection between the surface and the immobilized biomolecule, the sensing surface will become unstable, rendering it unsuitable for recurrent usage. [2], [29], [30].

Self-assembled monolayers (SAM) are one of the simple, commonly used methods in order to construct SPR sensor chips. Self-assembled monolayers (SAM) are a simple and widely used method for creating SPR sensor chips. The principle of molecular self-assembly of thiol or disulfide molecules at the metal surface underpins this approach. A SAM consists of a head group, tail, and functional end group. Some of the widely used head groups are thiols, silanes, phosphonates. While the head groups come together on the substrate, the tail groups direct upwards from the substrate. Thus, a densely packed and very stable structure is formed on the sensor surface. The terminal group of the molecule defines the surface properties of the SAM formed. Hydrophobic surfaces are formed by –CH3 and –CF3 terminal groups, while hydrophilic surfaces are formed by –COOH, –NH2, or –OH groups. SAMs can be deposited on metal substrates by immersing them in a dilute thiol/silane solution or by vapor deposition. These nanometer-thick SAMs can be simply produced from commercially available materials or at least relatively easily synthesized. The first applications of SAMs in biosensors were defined and developed in the late 1980s. Commercially available alkanethiols with various head groups for immobilizing

biological recognition components on biosensor surfaces include –COOH, –NH2, –OH, –biotin, and –N-hydroxysuccinimide. (NHS) [29], [30], [31].

The most popular commercial sensor chips on the market consist of a carboxymethylated dextran (CMD) matrix, which is made for Biacore AB. The unbranched glucose units of the dextran polymer give excellent flexibility and water solubility. Molecules can be covalently attached to the sensor surface through amine, thiol, aldehyde, or carboxyl functional groups present on the ligand. The carboxymethylated dextran matrix extends approximately 100 nm from the gold surface and is flexible, allowing relatively free movement of bound ligands [29], [31].

Today, graphene and its derivatives (graphene and reduced graphene oxide) have been utilized as potential detection platforms due to their superior properties such as biocompatibility and large surface areas non-toxicity, enriched functional groups, and excellent optical, electrical, and mechanical properties. Graphene is a monatomic thin planar layer composed of sp2 carbon atoms perfectly arranged in a honeycomb geometry. It is a good material for the interactions of biomolecules due to its rich conjugation structures. They can be easily applied and reused and are therefore widely used in biosensors [32], [33].

The non-specific adsorption degree of the SPR sensor interface determines the sensitivity and specificity of a biosensor. Effects such as hydrophobicity and hydrophilicity, surface charge, and pH are necessary to reduce non-specific adsorption at the sensor surface. Non-specific binding can lead to errors in concentration determination and calculation of kinetic constants. Creating hydrophilic interfaces can reduce non-specific binding on the sensor surface. Polymers are anti-fouling materials with their hydrophilic or zwitterionic nature, contributing to a reduction in non-specific protein adsorption. Hydrophilic polymers such as dextran, alginic acid, pectin, carboxymethyl cellulose, carboxymethyl dextran, polyglycerol, polyethylene glycol, poly-L-lysine, or polyacrylic acid are used on the SPR sensor surface [29], [34].

Polydopamine is a biomimetic adhesive material that can be easily applied to different surfaces and allows biomolecules to be easily attached to the surface through their amino and thiol groups without any coupling agent. Also, varying the deposition time can control the thickness of the polydopamine layer. It is an exciting material due to its attractive and straightforward properties in creating effective surface chemistry for SPR analysis. PDA coated surfaces have been recommended in various fields such

as cell adhesion, controlling the wettability of surfaces, anti-biological contamination surface, and biosensors.

Dopamine (DA) is known as a neurotransmitter, which plays an essential role in the mammalian central nervous system, is existed in mussel adhesive proteins. Formation of covalent and non-covalent bonds, DA self-polymerizes in an alkaline environment and forms a thin adhesive polydopamine (PDA) film that can adhere to surfaces. Polydopamine can be coated on almost any material surface: noble metals (Au, Ag, Pt, and Pd), metals with native oxide surfaces (Cu, stainless steel), oxides (TiO_2, SiO_2), semiconductors, ceramics, and synthetic polymers. The presence of functional groups as catechol and quinone provides that PDA can quickly and firmly adhere to surfaces. It is especially capable of covalently bonding with biomolecules that terminated with nucleophile groups such as amine- ($R\text{-}NH_2$) and thiol- ($R\text{-}S^-$) via Schiff base formation Michael addition reactions (Figure 2.8). Therefore, PDA is an exciting biomaterial for protein immobilization on solid surfaces [5], [6] [8], [29], [35].

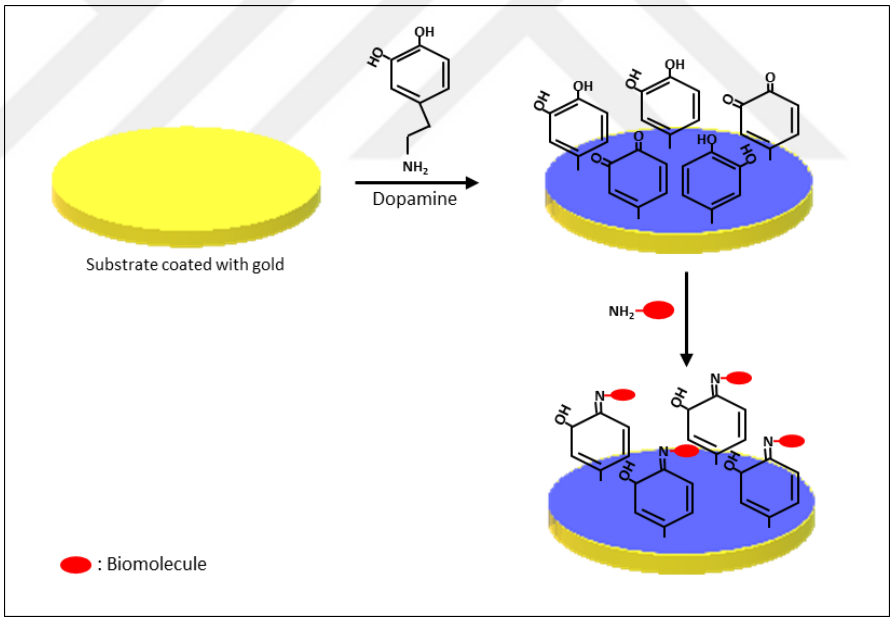

Figure 2.8: Illustration of PDA deposition and binding of biomolecules onto the PDA surface.

3. MATERIALS AND METHODS

3.1. Materials

Dopamine hydrochloride, Tris(hydroxymethyl)aminomethane (Tris), and Bovine serum albumin were obtained from Sigma-Aldrich. Phosphate buffered saline (PBS) (1x, pH 7.2) was received from Gündüz Kimya. Thermal evaporator system (Univex 450, Germany) was employed for gold coating. Spectroscopic ellipsometer (Semiconsoft MProbe, USA) was used to measure the thicknesses of PDA films. For SPR measurement, the SPR Imager device (NanoDev Scientific, Turkey) was used. CAM200 contact angle meter (KSV, Finland) was used for contact angle measurements. Microscope images were taken by Eclipse LV 150L (Nikon, Japan).

3.1.1. Preparation of Gold-coated Chips

Glass slides in circle shape to be used as chip sensors were 15 mm in diameter and 0.18 mm in thickness. Before the gold coating process, the glass slides were cleaned in acetone and isopropyl alcohol, followed by the oxygen plasma process subjected for 4 minutes. After the cleaning process, the glass slides were placed in the thermal evaporator coating system. 2 nm thick chromium (Cr) was primarily deposited on the glass slides as an adhesion layer. Then they were coated with gold (Au) in 50 nm thickness (Figure 3.1).

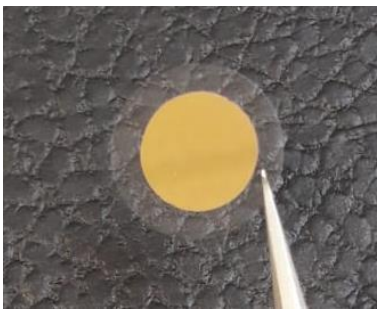

Figure 3.1: Au coated SPR chip. The diameter of Au coated area is 10 mm.

3.1.2. Preparation of Solutions

Polydopamine hydrochloride was dissolved in Tris buffer (pH 8.5, adjusted with NaOH) by stirring on magnetic stirring at 500 rpm at room temperature for 1 hour. The PDA deposition solution was obtained at a concentration of 2.0 mg/mL.

The BSA solution was prepared in PBS buffer by inverting up-down at concentrations of 12.5, 25, and 50 µg/mL.

3.1.3. Deposition of PDA films

Before the PDA deposition, gold coated chips were ultrasonically cleaned as immersing into acetone, isopropyl alcohol, and acetone for 5 minutes, respectively. PDA film was grown on a gold chip using an apparatus (Figure 3.2). A freshly prepared PDA deposition solution was used at ambient atmosphere. Varying the deposition time (30 min, 1hr, 1hr x 3 times, 24hr, and 3 days) controlled the PDA film thicknesses on SPR sensor. The thicknesses of PDA films were measured by spectroscopic ellipsometry device.

Figure 3.2: PDA deposition apparatus.

3.2. Characterization Methods

3.2.1. Measurement of PDA Film Thickness

Thicknesses of PDA films on the sensor chips were measured by Semiconsoft MProbe spectroscopic ellipsometry (Figure 3.3). Measurements were taken in the wavelength range of 400-1000 nm, average values were recorded.

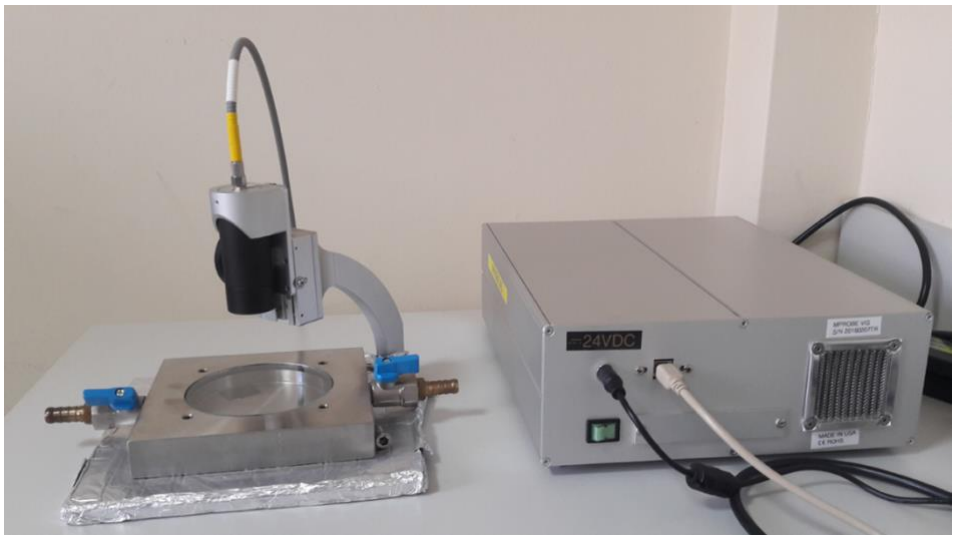

Figure 3.3: Semiconsoft MProbe spectroscopic ellipsometry device.

3.2.2. Contact Angle Measurement

Contact angle measurements were performed with KSV CAM200 contact angle meter (Figure 3.4). Contact angle is a method used in the characterization of solid surfaces based on measurement of the wettability of a solid by a liquid. Contact angles of non-PDA deposited and PDA deposited chips were taken, separately.

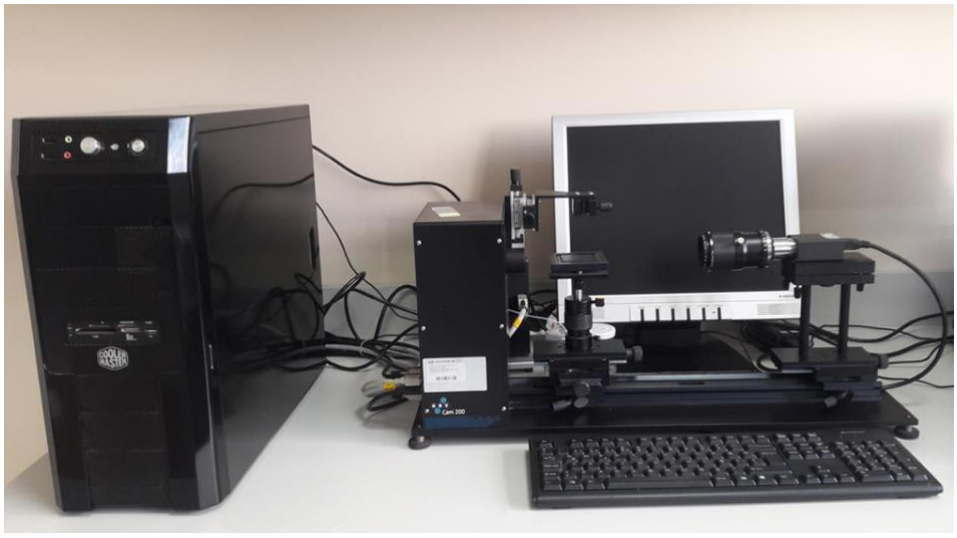

Figure 3.4: KSV CAM200 contact angle meter.

3.2.3. Microscope Images

Microscope images were taken by Nikon Eclipse LV 150L (Figure 3.5). Surface images of PDA-deposited sensor chips which are 200X and 500X zoomed were taken.

Figure 3.5: Nikon Eclipse LV 150L microscope images device.

3.2.4. Atomic Force Microscopy

Atomic force microscopy (AFM) images were collected by the AFM instrument (SPM-9600, Shimadzu) using a tapping mode.

3.3. SPR measurements

In this thesis, the SPR Imager device (NanoDev, Ankara, Turkey) was used. The SPR device consists of a diode (LED) light source that emits light at 850 nm wavelength. Figure 3.6 presents the N-BK7 glass (n = 1.51) prism integrated with the device equipment, O-ring, and the top view of the SPR chip combined with the equipment. Immersion oil (n=1.51) was dropped onto the prism to equalize the refractive index between a prism and sensor chip and prevent optical transmission loss. Followed by, the sensor chip was placed on the center of the prism, and then the sensor

chip was entrenched with a screw after O-ring was placed on the sensor chip to prevent liquid leakage.

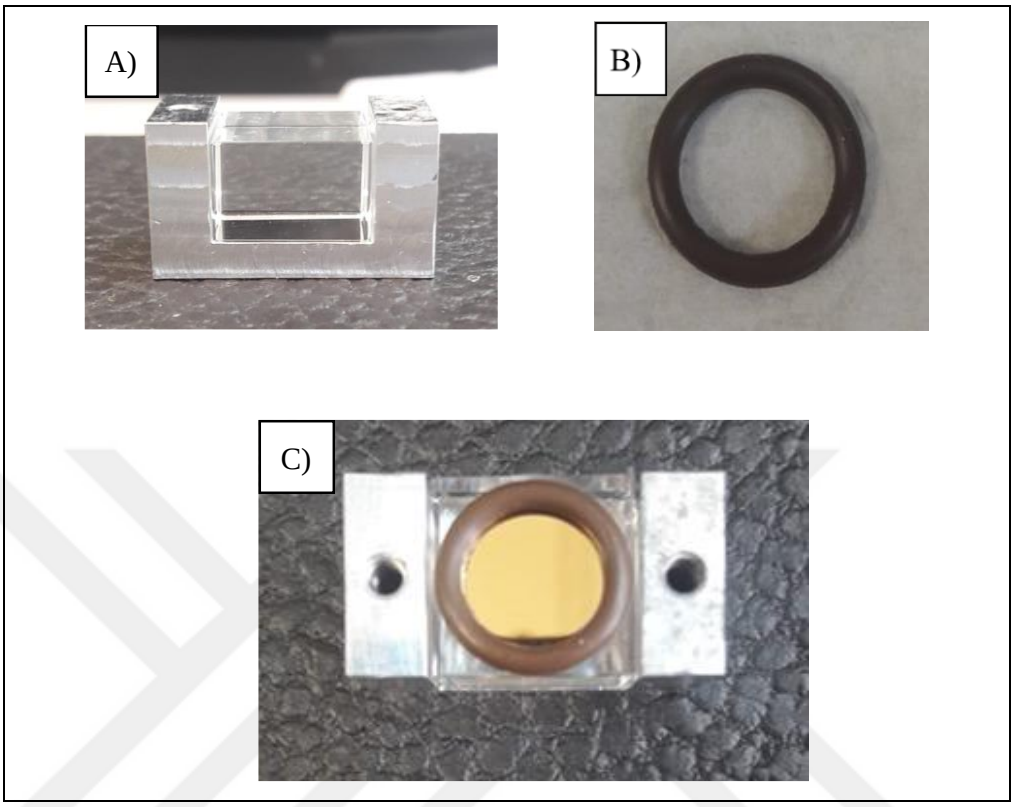

Figure 3.6: a) BK-7 glass prism, b) O-ring, c) integrated SPR equipement.

Figure 3.7 shows the experimental setup. We used a syringe pump to deliver the sample solution (BSA solution) onto the chip surface. The experiments were performed at room temperature. After the PDA deposition onto the sensor chips, SPR measurement was done immediately. The kinetics of protein attachment on PDA thin film were investigated in real-time. During the detection, to establish a steady baseline, PBS buffer was pumped through the sensor surface at a steady rate of 150 µL/min. The protein solution was then injected onto the sensing surface via a sample loop at a flow rate of 50 µL/mL, followed by washing with PBS buffer at the same rate. Lastly, the chip surface was regenerated by removing a 10 mM NaOH regeneration buffer at a 500 µL/mL flow rate. The changes at the resonance angle were monitored in real-time by the SPR software. The rise in the SPR response (degree) observed in PBS solution before and after protein solution injection was used to quantify the surface density of adsorbed proteins.

Figure 3.7: NanoDev SPR Imager device.

4. RESULTS

PDA film was grown on gold-coated sensor chips at different deposition times as 30 min, 1h, 1hr x 3 times, and 3 days to obtain different PDA film thicknesses. The thicknesses of PDA films were measured by spectroscopic ellipsometry. Table 4.1 indicates that the thicknesses of PDA films at various deposition time.

Table 4:1. The thickness change vs deposition time

Deposition time	Thickness (nm)
30 min	8
1 hour	15
3 hours	20
3 days	50

4.1. Contact Angle Measurement

Contact angle measurement is a practical surface characterization method of surfaces. The contact angle (wetting angle) is a measure of the wettability of a solid by a liquid. A liquid contacted with a solid surface forms a curve at a certain degree. Wetting (angle) provides information about the hydrophobicity of surfaces. When the contact angle is higher than 90º, the surface has a hydrophobic feature; on the other hand, it is lower than 90º, the surface is hydrophilic.

KSV CAM200 contact angle meter was used to measure the contact angle of PDA films. The contact angle values of bare gold and PDA films (Figure 4.1) and 8 nm, 15 nm, 20 nm, and 50 nm thicknesses (Figure 4.2) were that 82º, 75º, 72º, 67º, and 58º, respectively. The results shows that the increase in thickness improved the hydrophobicity. Figure 4.3 shows the bar chart diagram for the average contact angle values of the PDA films.

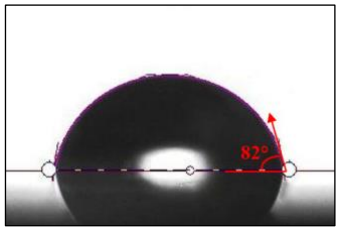

Figure 4.1: Contact angle of bare gold chip.

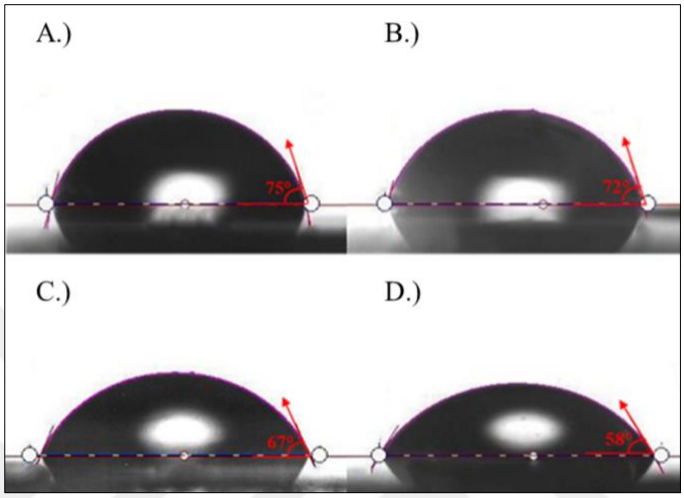

Figure 4.2: Contact angles of SPR chip modified by PDA films: a) 8 nm PDA, b) 15 nm PDA, c) 20 nm PDA, and d) 50 nm PDA.

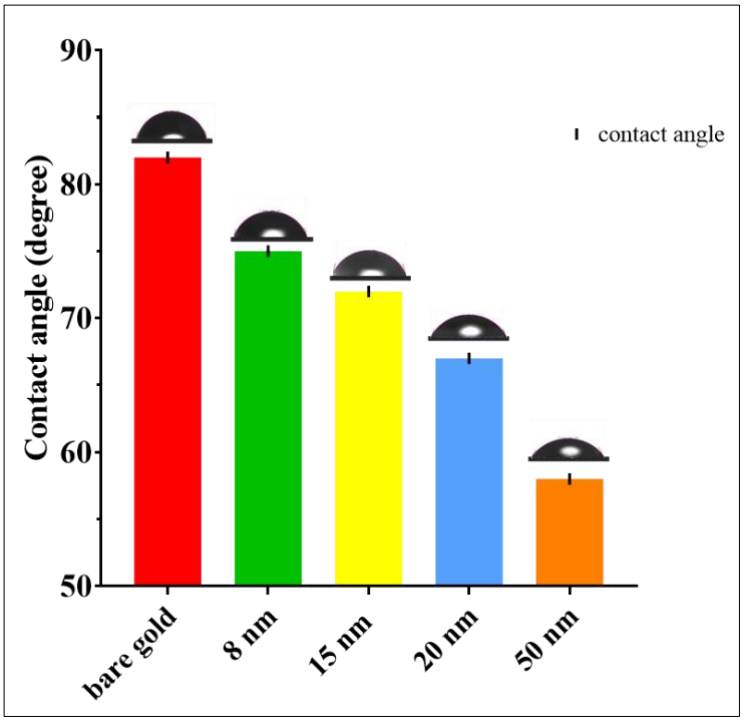

Figure 4.3: Bar chart diagram for the average contact angle values of the PDA films.

4.2. Microscope Images

Microscope images were taken of PDA films at 500X zoom by Nikon Eclipse LV 150L microscope. As seen in Figure 4.4, more PDA aggregates appeared on the chip surface when the deposition time increased. Also, particle size grew up, and the number of particles increased.

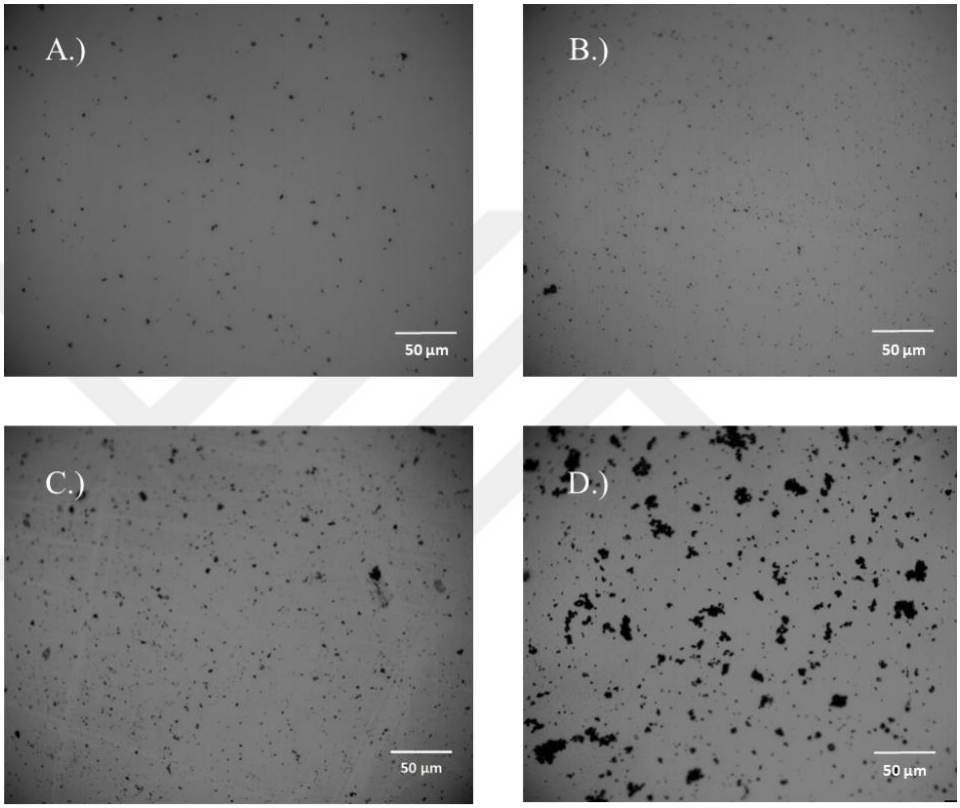

Figure 4.4: Microscope images of various thicknesses of PDA films. a) 8 nm PDA, b) 15 nm PDA, c) 20 nm PDA, and d) 50 nm PDA.

4.3. Atomic Force Microscopy (AFM) Measurement

AFM images were obtained in contact mode (Figure 4.5). The scan range was 5.0 µm x 5.0 µm, and the scan rate was 1 Hz. Roughness average (Ra) was used to evaluate the surface roughness. The surface topography images of PDA films at different thicknesses were taken, and Ra values were calculated using the AFM software. After the PDA deposition, the roughness increased to a Ra value of 0.767 nm, 1.037 nm, and 2.801 nm for the PDA films at 8 nm, 20 nm, and 50 nm,

respectively. It is seen that the roughness of PDA films increased with extended deposition time.

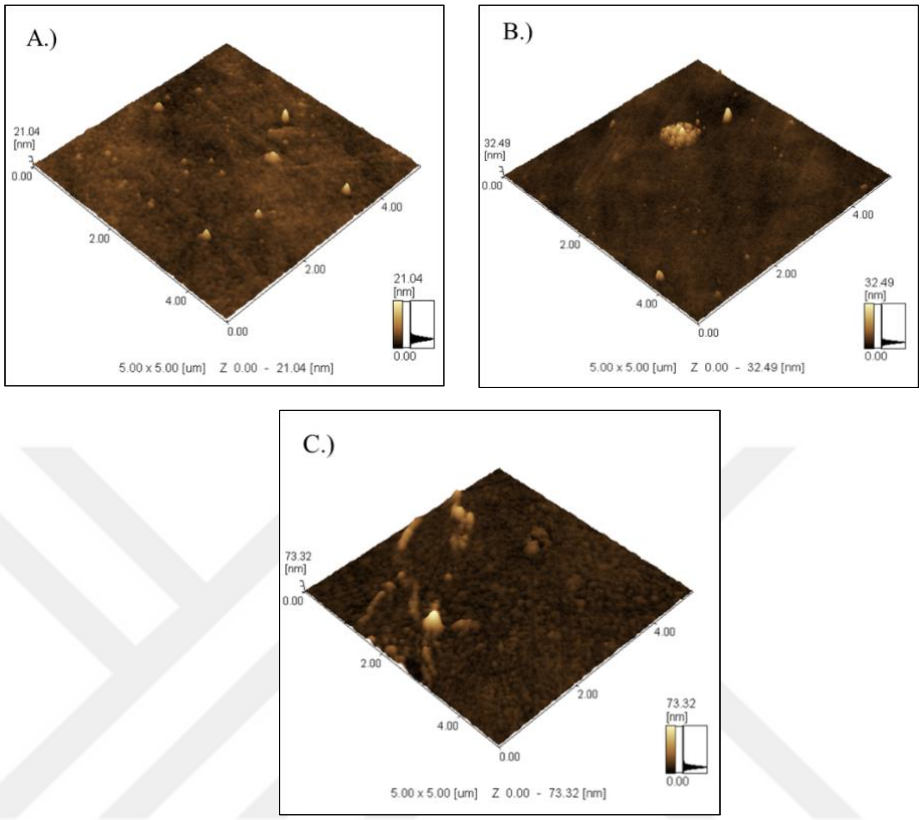

Figure 4.5: The AFM surface topographies of silicon modified by PDA films. a) 8 nm PDA, b) 20 nm PDA, c) 50 nm PDA.

4.4. SPR Measurement Analysis

SPR angles of these PDA deposited and bare gold-coated sensor chips were measured by delivering distilled water onto the sensor surface. SPR angle of bare gold-coated sensor chip was 64.88º. With the increase of PDA thicknesses, SPR angles were obtained as 65.83º, 66.40º, 67.60º, 71.84º and, 73.00º (Figure 4.6). SPR analysis results were demonstrated that the thickness of the PDA thin films has a significant effect on the SPR angle.

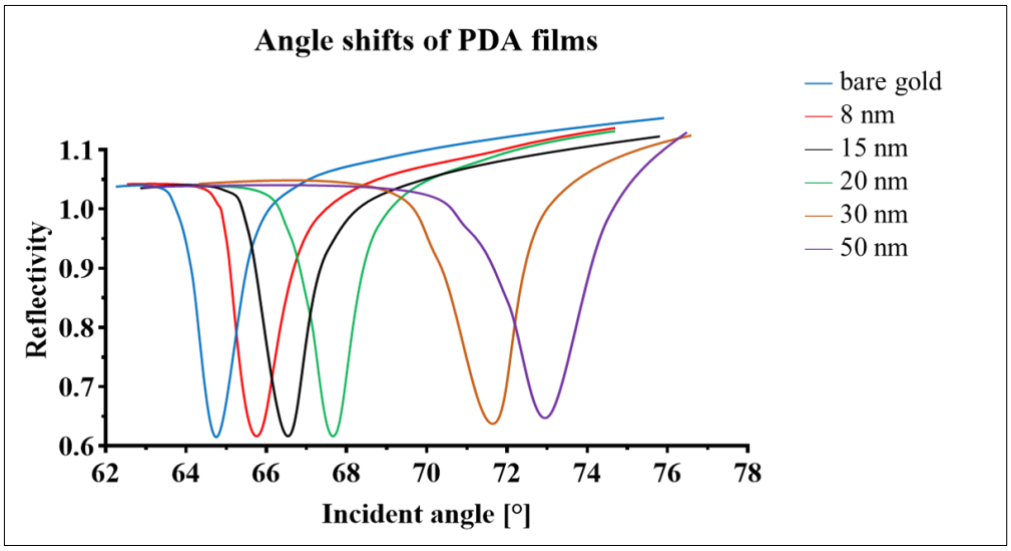

Figure 4.6: Angle shifts of different thicknesses PDA films.

4.5. Protein Binding SPR Analysis

Protein binding capabilities on PDA surface with different thicknesses were investigated. For this purpose, BSA was delivered with four different concentrations as 12.5 µg/mL, 25 µg/mL, 50 µg/mL, and 100 µg/mL onto the PDA films. BSA bindings were monitored to the PDA films.

First of all, it was investigated whether BSA bonded or not on a bare gold surface as a control sample. PBS was initially pumped through the sensor surface for 5 minutes to establish a steady baseline for the study. The protein solution was then administered at 50 g/mL and 100 g/mL concentrations. All solutions at different concentrations flowed through the sensor surface for 10 minutes. In the meantime, the software monitored changes in resonance angle in real-time. Figure 4.7 shows that the resonance BSA molecule did not bind on a bare gold surface.

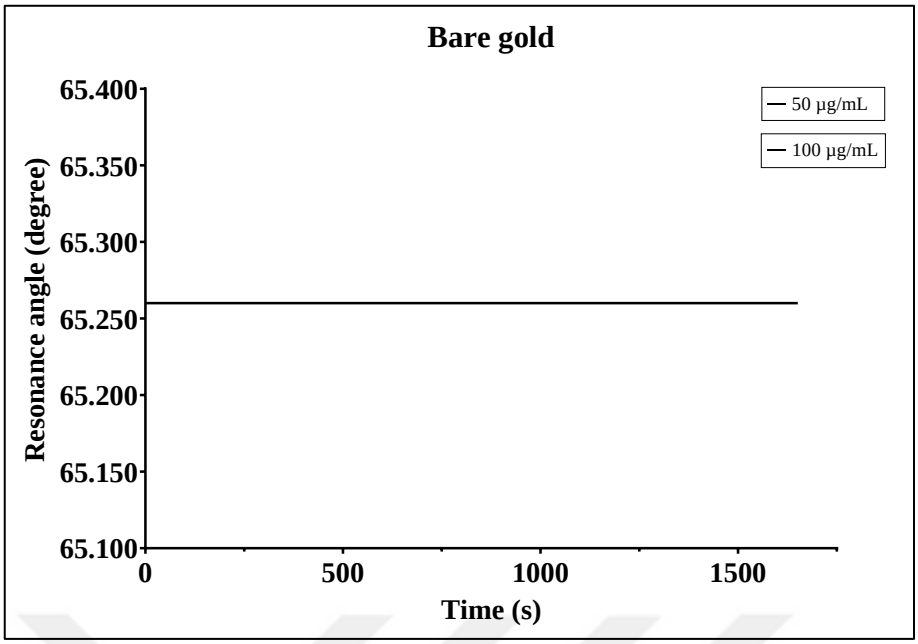

Figure 4.7: Binding curves of 50 µg/mL and 100 µg/mL BSA in situ on the bare gold chip.

BSA solutions of 12.5 µg/mL, 25 µg/mL, 50 µg/mL and 100 µg/mL concentrations were delivered onto the 8 nm PDA surface, and SPR signals were monitored. At 12.5 µg/mL, when the SPR signal reached baseline, the resonance angle was 66.420º. Followed by, BSA solution was injected onto the sensor surface and the resonance angle reached a value of 66.560º (Figure 4.8). According to the SPR analysis, an angle shift of 0.140º was observed.

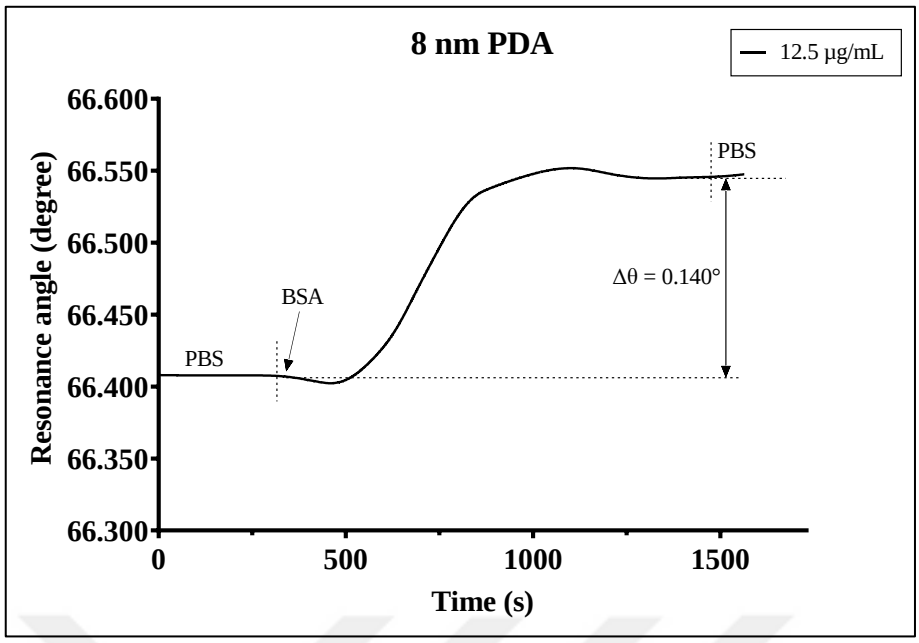

Figure 4.8: Binding curve of 12.5 µg/mL BSA in situ on the 8 nm PDA chip.

At 25 µg/mL, when the SPR signal reached baseline, the resonance angle was 66.402º. Followed by, BSA solution was injected onto the sensor surface and the resonance angle reached a value of 66.594º (Figure 4.9). According to the SPR analysis, an angle shift of 0.192º was observed.

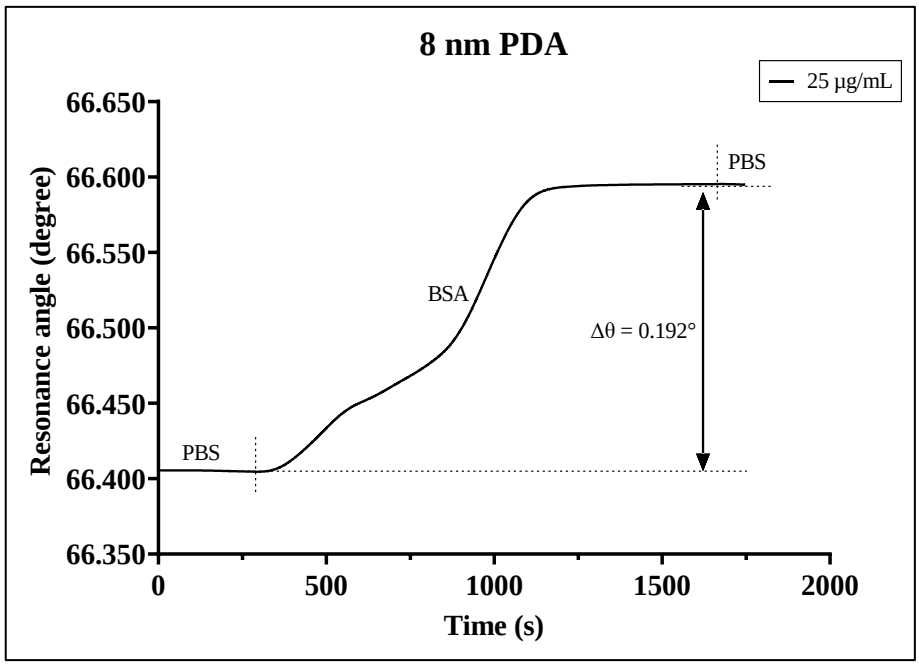

Figure 4.9: Binding curve of 25 µg/mL BSA in situ on the 8 nm PDA chip.

At 50 µg/mL, when the SPR signal reached baseline, the resonance angle was 66.644°. Followed by, BSA solution was injected onto the sensor surface and the resonance angle reached a value of 67.000º (Figure 4.10). According to the SPR analysis, an angle shift of 0.356º was observed.

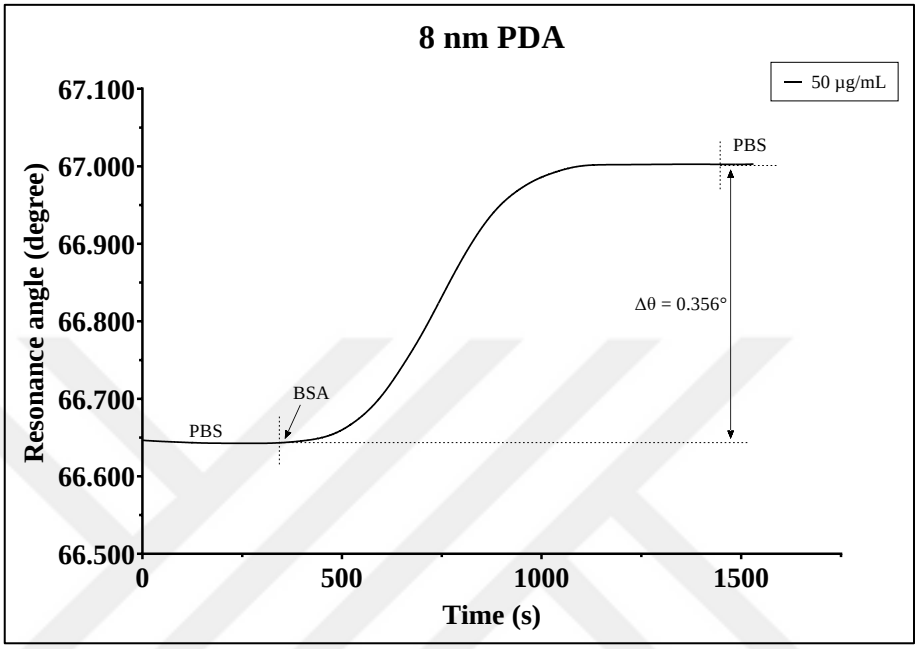

Figure 4.10: Binding curve of 50 µg/mL BSA in situ on the 8 nm PDA chip.

At 100 µg/mL, when the SPR signal reached baseline, the resonance angle was 65.940º. Followed by, BSA solution was injected onto the sensor surface and the resonance angle reached a value of 66.440º (Figure 4.11). According to the SPR analysis, an angle shift of 0.500º was observed.

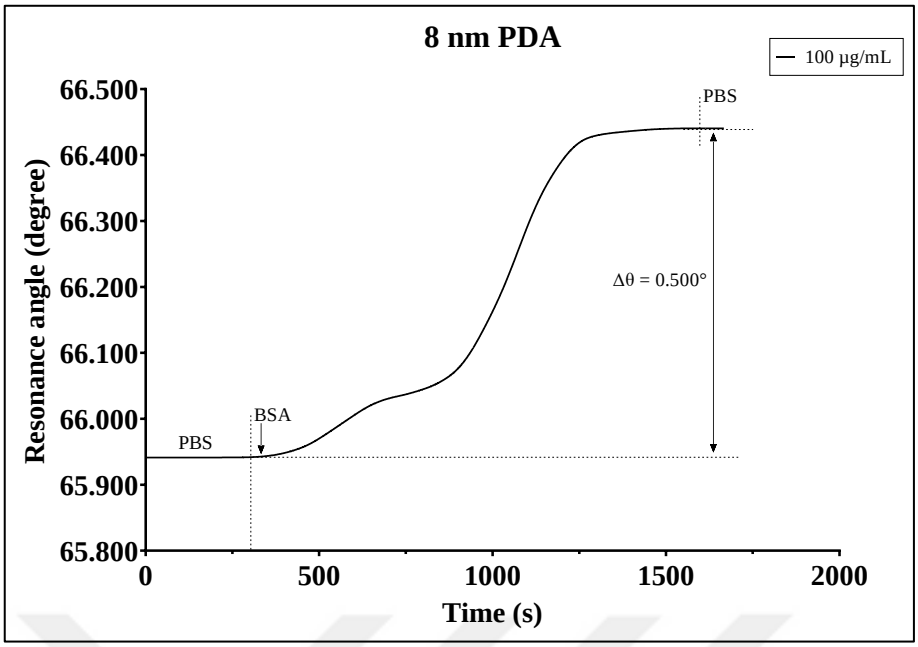

Figure 4.11: Binding curve of 100 µg/mL BSA in situ on the 8 nm PDA chip.

Figure 4.12 shows the association fitting curves of BSA concentration vs. SPR angle shift on the 8 nm PDA film obtained by SPR experiments. Higher BSA concentrations result in greater angle shifts, as can be shown. This behavior is attributed to the fact that a higher amount of proteins adsorbed on the PDA film surface with the higher protein concentrations.

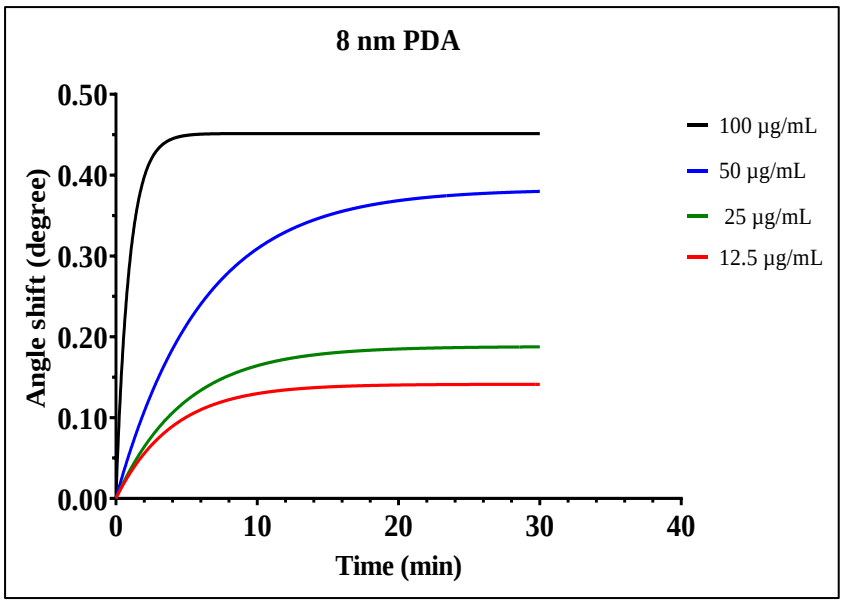

Figure 4.12: Association fitting curves of BSA with 100 µg/mL, 50 µg/mL, 25 µg/mL, and 12.5 µg/mL concentrations on 20 nm PDA film.

The protein attachment capability of PDA films was investigated for the thickness of 20 nm. At 25 µg/mL BSA, PBS was firstly delivered onto the sensor surface until the SPR signal reached baseline. The resonance angle was 68.678º when the SPR signal is in the baseline. Followed by, BSA solution was injected onto the sensor surface, and the resonance angle reached a value of 69.046º (Figure 4.13). According to the SPR analysis, an angle shift of 0.168º was observed.

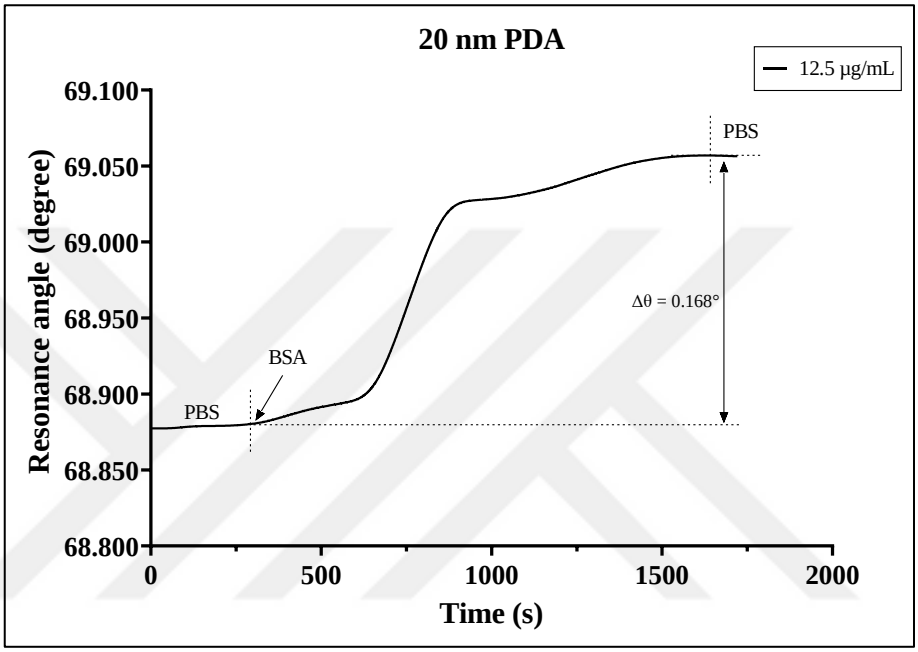

Figure 4.13: Binding curve of 12.5 µg/mL BSA in situ on the 20 nm PDA chip.

At 25 µg/mL BSA, PBS was firstly delivered onto the sensor surface until the SPR signal reached baseline. The resonance angle was 68.744º when the SPR signal is in the baseline. Followed by, BSA solution was injected onto the sensor surface, and the resonance angle reached a value of 68.958º (Figure 4.14). According to the SPR analysis, an angle shift of 0.214º was observed.

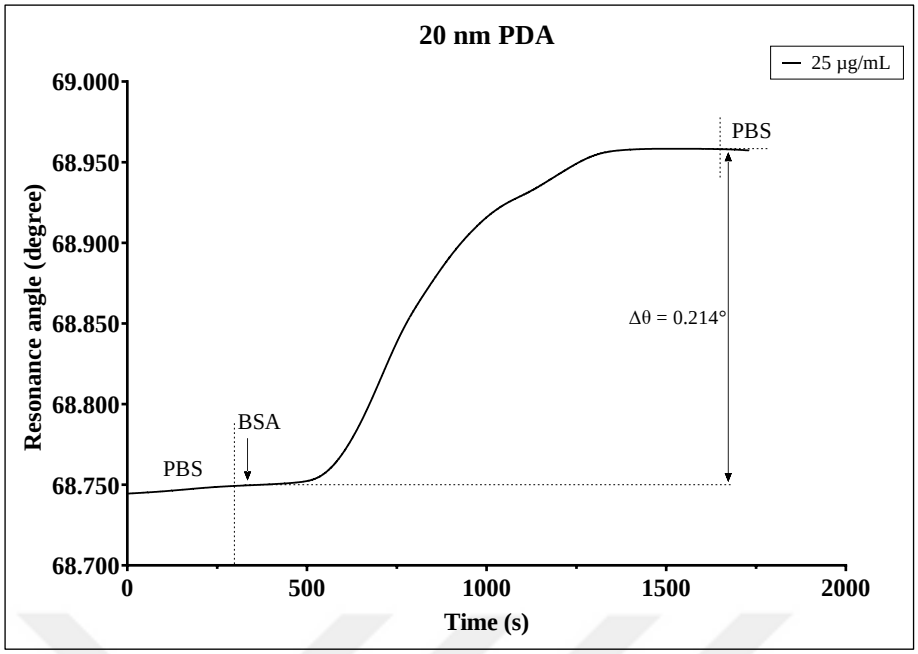

Figure 4.14: Binding curve of 25 µg/mL BSA in situ on the 20 nm PDA chip.

At 50 µg/mL, PBS was delivered onto the sensor surface until the SPR signal reached baseline. The resonance angle was 67.970º when the SPR signal is in the baseline. Followed by, BSA solution was injected onto the sensor surface, and the resonance angle reached a value of 68.320º (Figure 4.15). According to the SPR analysis, an angle shift of 0.350º was observed.

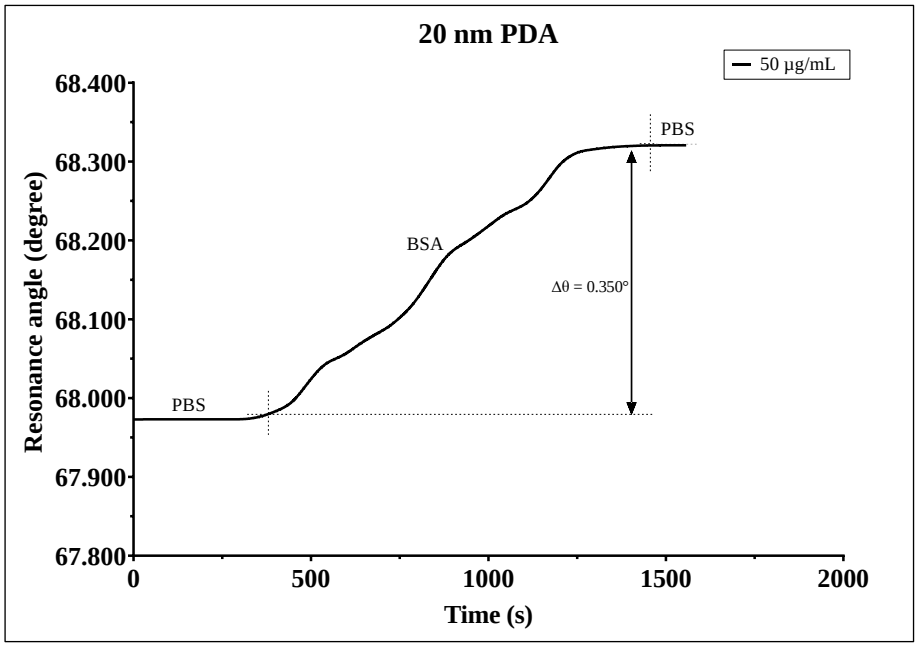

Figure 4.15: Binding curve of 50 µg/mL BSA in situ on the 20 nm PDA chip.

The protein adsorption capability of 50 nm PDA surface was also investigated. At 12.5 µg/mL BSA, PBS was delivered onto the sensor surface until the SPR signal reached baseline. The resonance angle was 73.644º when the SPR signal is in the baseline. Followed by, BSA solution was injected onto the sensor surface, and the resonance angle reached a value of 73.805º (Figure 4.16). According to the SPR analysis, an angle shift of 0.161º was observed.

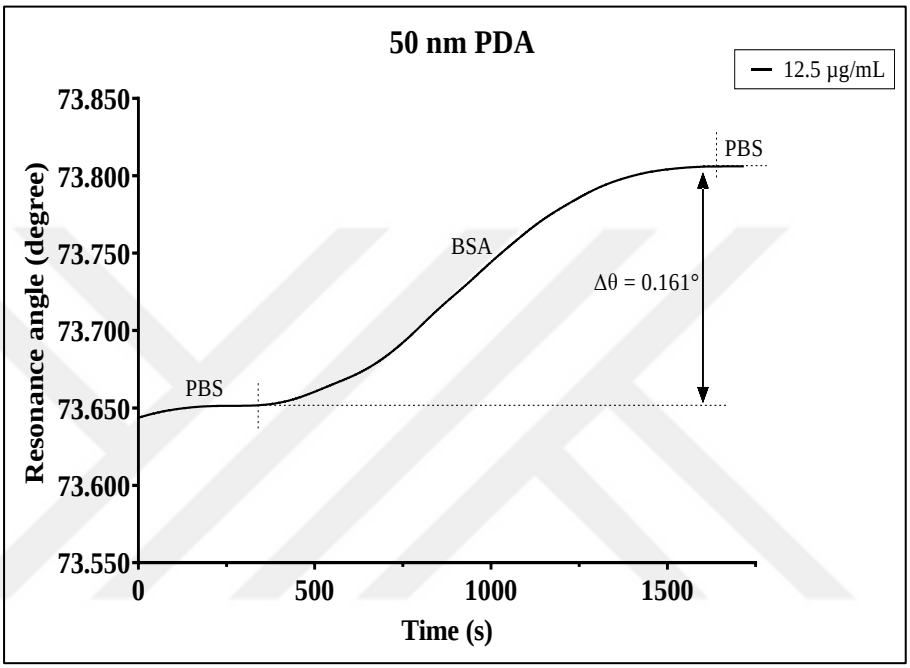

Figure 4.16: Binding curve of 12.5 µg/mL BSA in situ on the 50 nm PDA chip.

At 25 µg/mL BSA, PBS was delivered onto the sensor surface until the SPR signal reached baseline. The resonance angle was 73.470º when the SPR signal is in the baseline. Followed by, BSA solution was injected onto the sensor surface, and the resonance angle reached a value of 73.680º (Figure 4.17). According to the SPR analysis, an angle shift of 0.210º was observed.

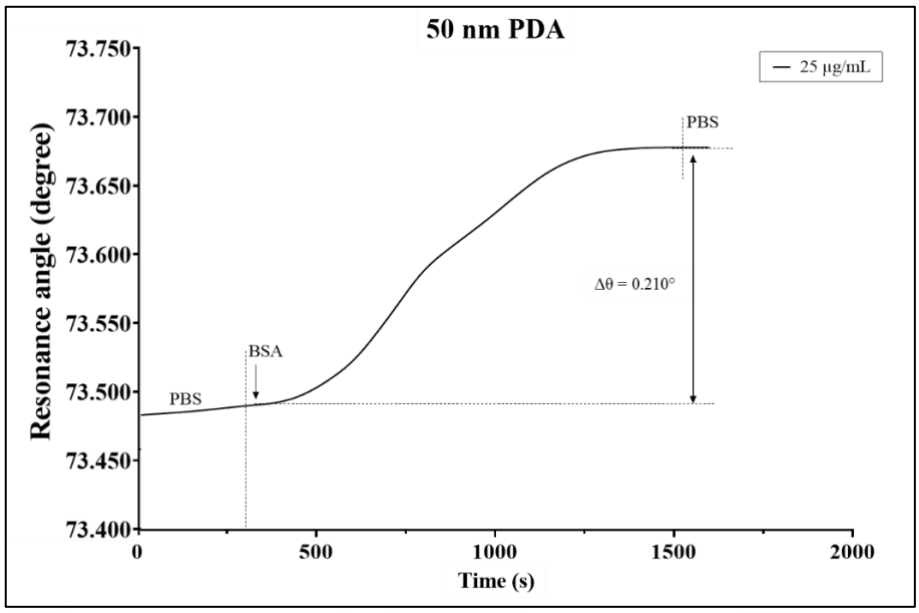

Figure 4.17: Binding curve of 25 µg/mL BSA in situ on the 50 nm PDA chip.

At 50 µg/mL BSA, PBS was delivered onto the sensor surface until the SPR signal reached baseline. The resonance angle was 73.360º when the SPR signal is in the baseline. Followed by, BSA solution was injected onto the sensor surface, and the resonance angle reached a value of 73.710º (Figure 4.18). According to the SPR analysis, an angle shift of 0.350º was observed.

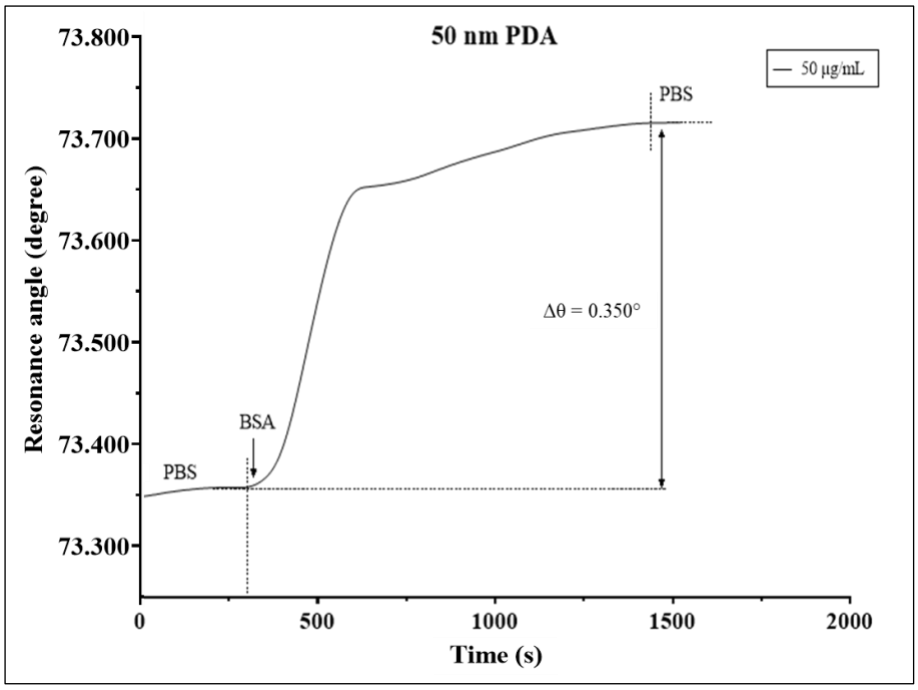

Figure 4.18: Binding curve of 50 µg/mL BSA in situ on the 50 nm PDA chip.

Summary of angle shifts of BSA binding onto the different thicknesses of PDA film is shown in the Table 4.2. There is no significant difference in protein binding capacity of 8 nm, 20 nm, and 50 nm PDA surfaces. At the 12.5 µg/mL and 25 µg/mL, the 20 nm PDA film gave the highest angle shift results. It means that a higher quantity of protein bind to the PDA surface. At 50 µg/mL, the 8 nm PDA film gave the highest shift result. However, this angle shift is not too higher than the 20 nm and 50 nm PDA films. The hypothesis of this study is thicker PDA layer with a higher surface area may increase the binding quantity of analytes, and the SPR signal may increase. In the light of the results, "thickness of PDA film influences protein binding capability as far as 20 nm thickness" but Over 20 nm, there is no influence of the thickness of PDA film on the protein binding capability. In this regard, 20 nm PDA film is better on good angle shift (response), short deposition time, and usage. In terms of fast deposition time, greater reflectivity (resonance depth), and curve form, the 20 nm PDA film would be a good candidate (resonance width). At a layer thickness of 40 nm or greater, both the minimal reflectivity (resonance depth) and curve shape (resonance breadth) significantly rise, implying a drop in SPR signal-to-noise ratio when the local RI (refractive index) changes [8].

Table 4.2: Angle shifts of BSA binding onto the different thicknesses of PDA film.

BSA Concentration	**PDA Thickness**		
	8 nm	**20 nm**	**50 nm**
12.5 µg/mL	0.140º	0.168º	0.161º
25 µg/mL	0.192º	0.214º	0.210º
50 µg/mL	0.356º	0.350º	0.350º
100 µg/mL	0.500º	-	-

In addition, the reproducibility of BSA attachment on the PDA deposited sensor chip was investigated. There was a decline in the attachment of BSA on PDA film at the second and third steps of BSA binding. However, this reduction in the amount of BSA attached to the surface was not significant and could be assumed negligible (Figure 4.19).

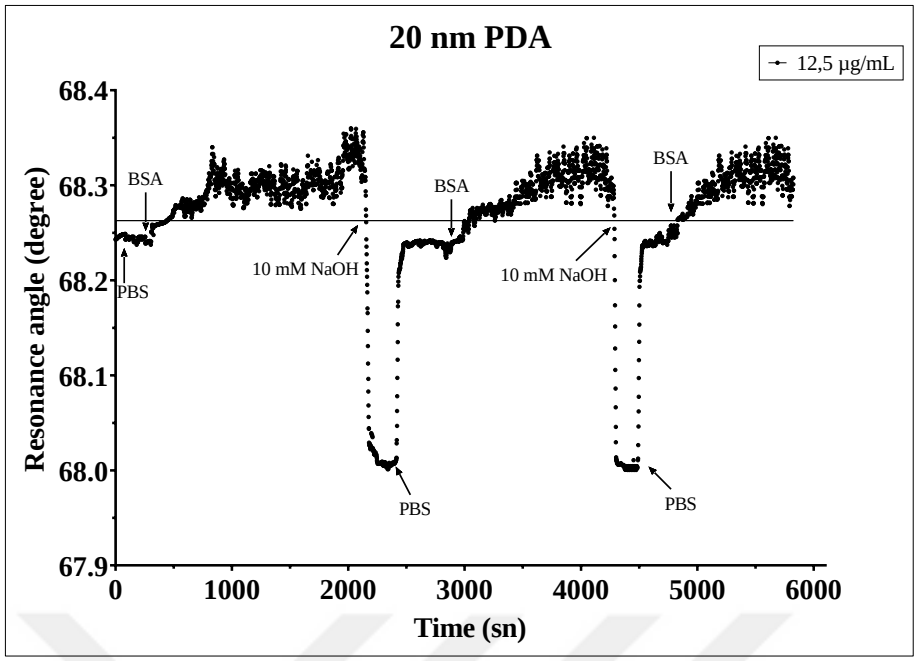

Figure 4.19: Reproducibility of BSA attachment on the PDA deposited sensor chip.

According to the SPR principle, amount of adsorption of protein on the surface is correlated to the SPR angle change with a ratio of 1 ng/mm^2 per 0.12 degree [5]. The final surface density of BSA on the 8 nm PDA film was calculated to be 4.17, 2.92, 1.6, and 1.3 ng/mm^2 respectively for 100, 50, 25, and 12.5 µg/mL BSA solution.

In addition, binding kinetics values of BSA were calculated by GraphPad Prism 8 software. Binding kinetics values of BSA were calculated for the each of PDA thicknesses. For the each of PDA thicknesses, binding kinetics was not very different each other. Therefore, standard deviation of binding kinetics were calculated as 2.33 x 10^{-10} M^{-1}.

5. CONCLUSIONS

In conclusion, this study was carried to understand dynamic of between PDA and protein interaction in detail. In situ research was conducted on the kinetics of protein immobilization on PDA film. Protein loading capacity of various PDA film thicknesses was found to be negligible. This study also showed that PDA film thickness increase when the deposition time is longer. Besides, the SPR angle degree increase depending on increased film thickness. This research could assist to clarify the ambiguity surrounding protein immobilization on PDA, expand our knowledge of the PDA-protein interaction, and provide a useful guidance for efficient protein attachment to PDA film in a variety of bio-related applications.

REFERENCES

[1] Guo X., (2014). "Fe3O4@Au nanoparticles enhanced surface plasmon resonance for ultrasensitive immunoassay", Sensors and Actuators B: Chemical, 205, 276-280.

[2] Gedig E. T., (2008), "Surface Chemistry in SPR Technology", Handbook of Surface Plasmon Resonance, RSC Publishing.

[3] Zhang Q., Jing L., Zhang J., Ren Y., Wang Y., Wang Y., Wie T., Liedberg B., (2014). "Surface plasmon resonance sensor for femtomolar detection of testosterone with water-compatible macroporous molecularly imprinted film", Analytical Biochemistry, 463, 7-14.

[4] Rahman M. S., Hossain B., Rana M., (2017). "Sensitivity enhancement of porous silicon based SPR sensor using graphene-M0S2 hybrid structure", IEEE.

[5] Toma M., Tawa K., (2016). "Polydopamine thin films as protein linker layer for sensitive detection of interleukin-6 by surface plasmon enhanced fluorescence spectroscopy", ACS Applied Materials & Interfaces, 8, 22032-22038.

[6] Wang N., Zhang D., Deng X., Sun Y., Wang X., Ma P., Song D., (2018). "A novel surface plasmon resonance biosensor based on the PDA-AgNPs-PDA-Au film sensing platform for horse IgG detection", Spectrochimica Acta Part A: Molecular and Biomolecular Spectroscopy, 191, 290–295.

[7] Yang W., Liu C., Chen Y., (2018), "Stability of polydopamine coatings on gold substrates inspected by surface plasmon resonance imaging", Langmuir, 34, 3565−3571.

[8] Chen D., Zahao L., Hu W., (2016), "Protein immobilization and fluorescence quenching on polydopamine thin films", Journal of Colloid and Interface Science, 477, 123–130.

[9] Karunakaran C., Rajkumar R., Bhargava K., (2015), "Introduction to Biosensors", Biosensors and Bioelectronics, Elsevier.

[10] Luong, J. H. T., Male, K. B., Glennon, J.D., (2008), "Biosensor technology: technology push versus market pull.", Biotechnol. Adv. 26 (5), 492-500.

[11] Lakshmipriya T., Gopinath S. C. B., (2019), "An Introduction to Biosensors and Biomolecules", Nanobiosensors for Molecular Targeting, Elsevier.

[12] Contreras-Naranjo J. E., Aguilar O., (2019), "Suppressing Non-Specific Binding of Proteins onto Electrode Surfaces in the Development of Electrochemical Immunosensors", Biosensors, 9, 15.

[13] Xie, B., Ramanathan, K., Danielsson, B., (1999), "Principles of enzyme thermistor systems: applications to biomedical and other measurements", Advances Biochemical Engineering, 64, 1-33.

[14] Evtugyn G., (2014), “Calorimetric Biosensors”, Biosensors: Essential, Springer.

[15] Jeong Y. Y., (2016), “Piezoelectric Sensors”, Introduction to Biosensors from The Electric Circuits to Immunosensors, 2nd Edition, Springer.

[16] Bard A. J., Faulkner L.R., (2001), Electrochemical methods Fundamentals and Applications, 2nd edition, Wiley and Sons Inc.

[17] Marazuela M. D, Moreno-Bondi M. C., (2002), “Fiber-optic biosensors-an overview”, Analytical and Bioanalytical Chemistry, 372, 664–682.

[18] Tudos A. J. and Schasfoort R. B. M., (2008), “Introduction to Surface Plasmon Resonance”, Handbook of Surface Plasmon Resonance, RSC Publishing.

[19] Mirabella, F. M. and Harrick, N.J., (1985), “Internal Reflection Spectroscopy: Review and Supplement”, Harrick Scientific Corporation, vol 3.

[20] de Mello A. J., (1996) “Surface Analytical Techniques for Probing Biomaterial Processes”, Davies, J., Ed., CRC Press, Boca Raton, New York, vol 1.

[21] Markey F., (1999), “What is SPR anyway?” Biajournal, 6, 14–17.

[22] Wilson W. D., (2002), “Analyzing biomolecular interactions”, Science, 295, 2103–2105.

[23] Drescher D. G., Selvakumar D., Drescher M. J., (2018), “Analysis of protein interactions by surface plasmon resonance”, Advances in Protein Chemistry and Structural Biology, 110, 1-30.

[24] Saito D., and Nakagawa T., (2020), “Chapter-20 Surface plasmon resonance”, Biomarkers for Traumatic Brain Injury, Academic Press.

[25] Douzi B., (2017), “Protein-Protein Interactions: Surface Plasmon Resonance”, Methods in Molecular Biology, Clifton, N.J., 1615, 257-275.

[26] Karlsson R., (2013), “Chapter 2.12 - Surface Plasmon Resonance in Binding Site, Kinetic, and Concentration Analyses”, The Immunoassay Handbook, 4th edition, Elsevier.

[27] O’Shannessy D. J., Brigham-Burke M., Soneson K. K., Hensley P., Brooks I., (1993), “Determination of Rate and Equilibrium Binding Constants for Macromolecular Interactions Using Surface Plasmon Resonance: Use of Nonlinear Least Squares Analysis Method”, Analytical Biochemistry, 212, 457-468.

[28] Ritzefeld M. and Sewald N., (2011), “Real-Time Analysis of Specific Protein-DNA Interactions with Surface Plasmon Resonance”, Journal of Amino Acids, 2012, 1-19.

[29] Hinman S. S., McKeating K. S., Cheng Q., (2018), “Surface Plasmon Resonance: Material and Interface Design for Universal Accessibility”, Analytical Chemistry, 90(1), 19-39.

[30] Altıntaş Z., Uludağ Y., Gürbüz Y., Tothill I., (2012), “Development of surface chemistry for surface plasmon resonance based sensors for the detection of proteins and DNA molecules”, Analytica Chimica Acta, 712, 138-144.

[31] Löfås S. and McWhirter A., (2006), “The Art of Immobilization for SPR Sensors”, Surface Plasmon Resonance Based Sensors, Springer.

[32] Omar N. A. S., Fen Y. W., Saleviter S., Daniyal W. M. E. M. M., Anas N. A. A., Ramdzan N. S. M., Roshidi M. D. A., (2019), “ Development of a Graphene-Based Surface Plasmon Resonance Optical Sensor Chip for Potential Biomedical Application”, Materials, 12 (12), 1928.

[33] Szunerits S., Maalouli N., Wijaya E., Vilcot J. P., Boukherroub R., (2012), “Recent advances in the development of graphene-based surface plasmon resonance (SPR) interfaces” Analytical and Bioanalytical Chemistry, 405(5), 1435-1443.

[34] Wijaya E., Lenaerts C., Maricot S., Hastanin J., Habraken S., Vilcot J. P., Boukherroub R., Szunerits S., (2011), “Surface plasmon resonance-based biosensors: From the development of different SPR structures to novel surface functionalization strategies”, Current Opinion in Solid State and Materials Science, 15, 208-224.

[35] Lee H., Dellatore S. M., Miller W. M., Messersmith P. B., (2007), “Mussel-Inspired Surface Chemistry for Multifunctional Coatings”, Science, 318, 426-430.

BIOGRAPHY

Özge Çelik completed her high school at Çamlıca Anadolu Kız Lisesi, İstanbul in 2013. Then, she obtained a Bachelor's degree in Genetics and Bioengineering at Kastamonu University in 2017. In her bachelor thesis, she studied “Biomimetic wound dressing design for the treatment of second-degree burns”. Afterward, she completed her Master's degree in The Institute of Biotechnology at Gebze Technical University, Kocaeli in 2021. In her master thesis, she studied “Investigation of polydopamine modification on surface plasmon resonance sensor chip for detection of biomolecules”. She did her internships in Microbiology Laboratory at Novartis, İstanbul in 2015, in Molecular Cell Biology Laboratory at Yeditepe University, İstanbul in 2016, in The Institute of Biomaterials at Friedrich Alexander University, Erlangen in 2017. Lastly, she worked as an intern at Roche Diagnostics GmbH, Penzberg in 2021, she worked on protein-protein interactions there.